THE UNIVERSITY OF CALGARY

Evaluation of Reovirus as an Oncolytic Agent in Malignant Gliomas

By

Mary Elizabeth Wilcox

A DISSERTATION SUBMITTED TO THE FACULTY OF GRADUATE STUDIES IN PARTIAL FULFILLMENT OF THE REQUIREMENTS LEADING TO A MASTER OF SCIENCE DEGREE

DEPARTMENT OF MEDICAL SCIENCE

CALGARY, ALBERTA

MAY, 2000

ABSTRACT

Reovirus is unlike other viral/gene therapy approaches. It differs from both the E1B gene-attenuated adenovirus (ONYX-015) that targets cancer cells lacking functional tumor suppressor protein p53 and the genetically altered herpes simplex virus (G207) that targets cancer cells with a dysfunctional p16/pRB tumor suppressor pathway as it is a naturally occurring unmodified oncolytic virus. This double-stranded RNA virus selectively infects and kills cells with Ras-activation leaving normal untransformed cells unharmed. Since Ras-activated pathways are present in the majority of malignant gliomas we were prompted to examine the potential usefulness of reovirus treatment for this form of cancer. Susceptibility of glioma cells to reovirus suggested that: (a) human glioma tumor cells are effectively killed within a 48 hour period by *in vitro* exposure to doses of 40 PFUs/cell in both established cell lines and *ex vivo* glioma specimens; (b) reovirus effectively reduced tumor volume *in vivo* in both subcutaneous and intracerebral SCID NOD models, in most instances curing these mice; (c) reovirus caused tumor regression in the presence of pre-existing anti-reovirus antibodies in immunocompetent Fischer rats; and (d) reovirus killed tumors remote from the site of administration in immunocompetent host. Considerable toxicity however was found with this viral approach when repeatedly administered intracerebrally in immunocompetent Fischer 344 rats. Wide spread encephalitis being the major problem with this approach. The potential short- and long-term effects of reovirus administration in the brain are under ongoing investigation. It remains to be determined if this toxicity can be reduced using different doses, schedules of administration, antibodies, etc. This study does show

nevertheless that reovirus has potent oncolytic activity against glioma tumors. Following modification of its brain toxicity, reovirus may be a candidate for clinical trials and use in combination with conventional therapies.

ACKNOWLEDGEMENTS

There are so many people that I wish to thank for their contributions to this dissertation, either for their direct assistance in the area of science or through less direct but certainly not less important areas of friendship and camaraderie. The first person that I would like to thank is Dr. Peter Forsyth, to whom I am indebted as he has granted me the privilege of studying in his laboratory for the last two years. For his time, patience and knowledge (that he so modestly shares) I am forever grateful.

I would also like to thank the members of my supervisory committee, Dr. Stephen Robbins, Dr. Voon Wee Yong and Dr. Patrick Lee for all their efforts and support. I would also like to thank Dr. Brian MacVicar for serving as the external examiner for my defense.

To members of our lab and the labs that adopted me "as their own", thank you for making school fun. I think that there will probably never be a more entertaining place to work. Thank you especially to Tammy Wilson, Zhong Qiao Shi, Sheetal Raithatha, Huong Muzik, Mike Nodwell, Lori Groft, Kara Norman, Dr. Matt Coffey, Dr. Jim Strong, Arnaud Besson, Duc Le, Fiona Yong, Shannon Corley, Tommy Alain, Peter Lewkonia, Chris Howlett, Dr. Geoff Pinchbeck, Dr. Wen Qing Yang, and anyone else I may have missed.

I am indebted to Eve Lee for helping me through deadlines and ensuring that all my applications were in order.

To my dear friends, Andrew Baxter, Jeremy Leyden, Jonah Shiu, Owen Craig and Ryan Ramage: thank you.

I am especially indebted to my family for getting me through the tough parts (and you are fully aware of when those were). Thank you for your love and support.

To my family,

a great man, David Fisher,

a dear friend, Christina Northcott.

TABLE OF CONTENTS

LIST OF FIGURES

LIST OF TABLES

LIST OF ABBREVIATIONS

ATCC = American Type Culture Collection

CO_2 = carbon dioxide

DMEM = Dublecco's modified eagle medium

ds = double-stranded

EDTA = ethylenediamine tetraacetic acid

EGF-R = epidermal growth factor – receptor

FA = fetal astrocytes

FBS = fetal bovine serum

FITC = fluorescein isothiocyanate

FN = fetal neurons

GBM = glioblastoma multiforme

GFAP = glial fibrillary acidic protein

H&E = hematoxylin and eosin

hr = hour

HRP = horse radish peroxidase

i.c. = intracerebral

i.p. = intraperitoneal

i.t. = intratumoral

i.v. = intravenous

ISVP = infectious subviral particle

JMEM = Joklik's minimum essential medium

JNK = c-jun N-terminal kinase

LD_{50} = lethal dose 50%

MAPK = mitogen activated protein kinase

MEN = meningioma

mins = minutes

ml = milliliters

μl = microliters

MOI = multiplicity of infection

mRNA = messenger ribonucleic acid

PBS = phosphate buffered saline

PDGF-R = platelet derived growth factor – receptor

PKR = double-stranded RNA activated protein kinase

RNA = ribonucleic acid

rpm = revolutions per minute

SCID = severe combined immundeficent

SDS-PAGE = sodium dodecyl sulfate-polyacrylamide gel

T1L = type 1 Lang

T2J = type 2 Jones

T3D = type 3 Dearing

TGF-α = transforming growth factor – alpha

wk = week

+ = infected

- = mock-infected

CHAPTER 1. INTRODUCTION

1.1. REOVIRUS

1.1.1. Classification

The Reoviridae are a family of non-enveloped, icosahedral, double-shelled viruses containing segmented, double-stranded RNA genomes. It consists of 3 genera associated with mammalian disease: rotavirus, orbivirus and reovirus (Tyler and Fields, 1990). While the clinical importance of rotavirus is well established, the importance of reoviruses as etiological agents in human disease is unclear.

Reoviruses (respiratory enteric orphan virus) are common isolates of the respiratory and gastrointestinal (GI) tract of humans but they are not associated with any known disease state and are therefore considered benign (Sabin, 1959). The human reoviruses are among the best-characterized members of the reoviridae family (Table 1). They consist of three distinct serotypes based upon antibody neutralization and hemagglutination inhibition tests: Type 1 (strain Lang; T1L), Type 2 (strain Jones; T2J) and Type 3 (strain Dearing; T3D) (Rosen, 1960). Each virus type has its own characteristic features including differential effects on host cell RNA and protein synthesis. Typically, reovirus type 1 affects host macromolecular synthesis very little, type 2 causes rapid and almost complete inhibition of host synthesis and type 3 results in an intermediate level of restriction of host synthesis later in infection (Joklik, 1985). Type 2 reovirus inhibits L929 cell RNA and protein synthesis more rapidly and efficiently then type 3 (Sharpe and Fields, 1982; Joklik 1985). Each serotype has been demonstrated to possess distinct patterns of tissue tropism and viral spread in infected hosts (Tyler and Fields, 1990).

Despite high antibody prevalence, the majority of individuals have detectable antibodies against reoviruses of all three serotypes by the time they leave childhood (Nibert et al., 1996). The reoviruses however appear not to be the major causes of symptomatic

TABLE 1. PROPERTIES OF THE MAMMALIAN REOVIRUSES

Genome

- Double-stranded RNA
- 10 gene segments in three size classes
- Total size 23,500 base pairs
- Gene segments encode either one or two proteins each
- Gene segments are transcribed into full-length mRNAs
- Plus strands of gene segments have 5' caps
- Nontranslated regions at segment termini are short
- Gene segments can undergo reassortment between virus strains

Particles

- Spherical, with icosahedral (5:3:2) symmetry
- Nonenveloped
- Total diameter 85 nm (excluding σ1 fibers)
- Two concentric protein capsids: outer capsid subunits in T=13 lattice, arrangement of inner capsid subunits unknown
- 8 structural proteins: 4 proteins in outer capsid (λ2, μ1 [mostly as cleavage fragments μ1N and μ1C], σ1, and σ3) and 4 proteins in inner capsid (λ1, λ3, μ2, and σ2)
- Subviral particles (ISVPs and cores) can be generated from fully intact particles (virions) by controlled proteolysis
- Cell-attachment protein σ1 can extend from the virion and ISVP surface as a long fiber
- Protein λ2 forms pentamers that protrude from the core surface

Replication

- Fully cytoplasmic
- Sialic acid can serve as cell surface receptor for recognition by cell-attachment protein σ1
- Proteolytic processing of outer capsid protein σ3 and μ1/μ1C is essential to infection and can occur either extracellularly or in endo/lysosomes
- Uncoating of parent particles is incomplete: genomic dsRNA does not exit particles to enter the cytoplasm
- Transcription and capping of viral mRNAs occur within particles and are mediated by particle-associated enzymes
- Segment assortment and packaging involves mRNAs
- Minus-strand synthesis occurs within assembling particles
- Mature virions are inefficiently released from infected cells by lysis

(Nibert et al., 1996)

disease. They are most probably associated with upper respiratory infections as well as enteritis in infants and children (Nibert et al., 1996). Upon inoculation of human adult volunteers with reovirus, symptoms such as cold and flu-like symptoms of cough, sneezing, pharyngitis, rhinorrhea, malaise and headache were observed in 4 of 27 subjects (Rosen et al., 1960). Other studies have indirectly linked reovirus with such infections as encephalomyelitis, meningioencephalitis, motor neuron disease, pneumonitis, keratoconjunctivitis, and asymptomatic viruria. Though these cases are poorly documented they represent single case reports and only describe associations (Tyler and Fields, 1990).

1.1.2. Structure of reovirus

The genome of the mammalian reoviruses consists of ten segments of dsRNA divided into three size classes as determined by their migration on gel electrophoresis (Shatkin et al., 1968; Bellemy and Joklik, 1967). These segments are designated large (segments L1, L2 and L3), medium (segments M1, M2 and M3) and small (segments S1, S2, S3 and S4) (Joklik, 1985). Homologous segments from different isolates including prototypes of the three serotypes often exhibit differences in their electrophoretic mobilities (Ramig et al., 1983). The fact that reoviruses have segmented genomes has important biological and experimental consequences as they are able to exchange gene segments between isolates within a genus and thereby generate reassortant progeny viruses. All of the genes from prototypes strain T3D (encompassing 23,549 base pairs in total; Wiener et al., 1989) have now been sequenced either from cDNAs (Cashdollar et al., 1989; Cashdollar et al., 1982; Imai et al., 1983) or directly from genomic RNA (Bassel-Duby et al., 1986).

The proteins encoded by these RNA segments, also grouped according to size, correspond to the large or λ polypeptides (λ1, λ2, and λ3), medium or μ polypeptides (μ1, μ2, and μns) and the small segments or σ polypeptides (σ1, σ2, σ3 and σns) (Nibert et al., 1996). Eight of these eleven proteins comprise structural proteins included in the infecting virus particle. The three remaining proteins (σ1s, σns and μns) represent non-structural entities present only in the infected cell's cytoplasm. The major constituents of

the inner capsid are λ1, λ2, and σ2. The three minor constituents are λ3, μ1 and μ2 (Joklik, 1985). The outer capsid consists of the two major proteins, σ3 and μ1c (a cleavage product of the core protein, μ1) as well as the minor protein σ1 (also serves as the virus attachment protein) (Lee et al., 1981). Although often considered a distinct structure the λ2 component of the inner capsid (often referred to as the core) extends outward to the surface of the outer capsid at each of the twelve vertices of the icosahedron. This allows for the formation of a structural linkage between the inner and outer capsids (Luftig et al., 1972).

1.1.3. Reovirus replication cycle

Attachment of the virion (or ISVP) to receptor molecules on the cell surface is the first step in reovirus infection (Figure 1; Tyler and Fields, 1996). Reovirus binds most mammalian cells; sialic acid is the cell surface receptor for recognition by cell-attachment protein σ1 (Choi et al., 1990; Paul et al., 1989; Gentsch and Pacitti, 1985; Gentsch and Pacitti, 1987). Virion particles are taken up from the cell surface following their attachment by receptor-mediated endocytosis. They are then delivered into vacuoles (endosomes/lysosomes) at which time reovirus outer capsid proteins undergo specific proteolytic cleavages (Tyler and Fields, 1996). These cleavages are acid-dependent and represent an essential step in the infection process. The mechanism by which reoviruses interact with and penetrate the vacuolar or plasma membrane barrier is unknown but appears dependent upon preceding proteolysis, as only the ISVP form exhibits membrane interaction in available assays (Tyler and Fields, 1996).

Following internalization, the "core particle" of the ISVP becomes transcriptionally active and begins synthesis of the ten-capped viral mRNAs following internalization (Tyler and Fields, 1996). The transcription and capping of viral mRNAs are mediated by particle-associated enzymes within these core particles (Nilbert et al., 1996). Primary transcripts are used for the translation of viral proteins by the cellular protein synthesis machinery (Tyler and Fields, 1996). Cellular protein synthesis machinery is "taken over" by the virus for translation of its proteins from primary transcripts. This inhibition of

host protein synthesis does not however appear early in infection but takes place gradually. It is not until late in infection that essentially all the proteins synthesized by the host are in fact viral (Zweerink and Joklik, 1970; Detjen et al., 1982; Munemitsu and Samuel, 1984; Munoz et al., 1985).

The association of early viral transcripts with newly made viral proteins results in the formation of progeny RNA assortment complexes. Within these replicase particles, each of the ten packaged plus strands serve as a template for minus strand synthesis (Tyler and Fields, 1996). Furthermore, these progeny subviral particles are involved in a secondary transcriptional event of viral mRNAs (secondary transcription). These "late" transcripts are reported to be uncapped and serve as the primary templates for viral protein synthesis during "late" infection (Tyler and Fields, 1996). It has been suggested that the shift from cell-specific to viral-specific protein synthesis late in infection is due to virus-induced alterations in the host translation machinery. The absence of a cap structure onto late mRNAs, compared with early viral mRNAs and cellular mRNAs, is believed to be involved in the shut down of host protein synthesis (reviewed by Zarbl and Millward, 1983; Lemay, 1988). The final steps of virion capsid assembly are not well defined. Mature virions undergo an inefficient process of release from infected cells following lysis (Tyler and Fields, 1996).

1.1.4. Neuropathogenesis of reovirus in neonates and immunodeficient mice

The reoviruses do not appear to be an important cause of symptomatic disease in human adults, however experimental infection of laboratory mice has been demonstrated to be associated with serotype-specific disease. The inoculation of neonatal mice with reovirus serotype 1 Lang results in a non-lethal ventriculitis followed by hydrocephalus resulting from reovirus infection of the ependymal cells (Sharpe and Fields, 1985; Tyler and Fields, 1996). Serotype 3 Dearing infection of neonates results in a fatal encephalitis due to the infection of neuronal cells (Sharpe and Fields, 1985; Tyler and Fields, 1996). Such an infection has been shown to cause extensive necrosis of the cortex associated in some

Figure 1.1. Reovirus replication cycle. The primary steps in replication are labeled (*bold capital letters*). Virions, ISVPs and cores as well as other assembly-related particle forms are indicated. Capped plus-stranded RNAs – as part of the ten dsRNA genome segments, as cytoplasmic-transcripts, and as assortment elements – are indicated (5'-terminal open *circles* represent caps). Uptake from the cell surface is shown to involve receptor-mediated endocytosis, with viral particles sequentially associated with clathrin-coated vesicles, endosomes, and lysosomes (the last three compartments are acidic, as shown; Tyler and Fields, 1996).

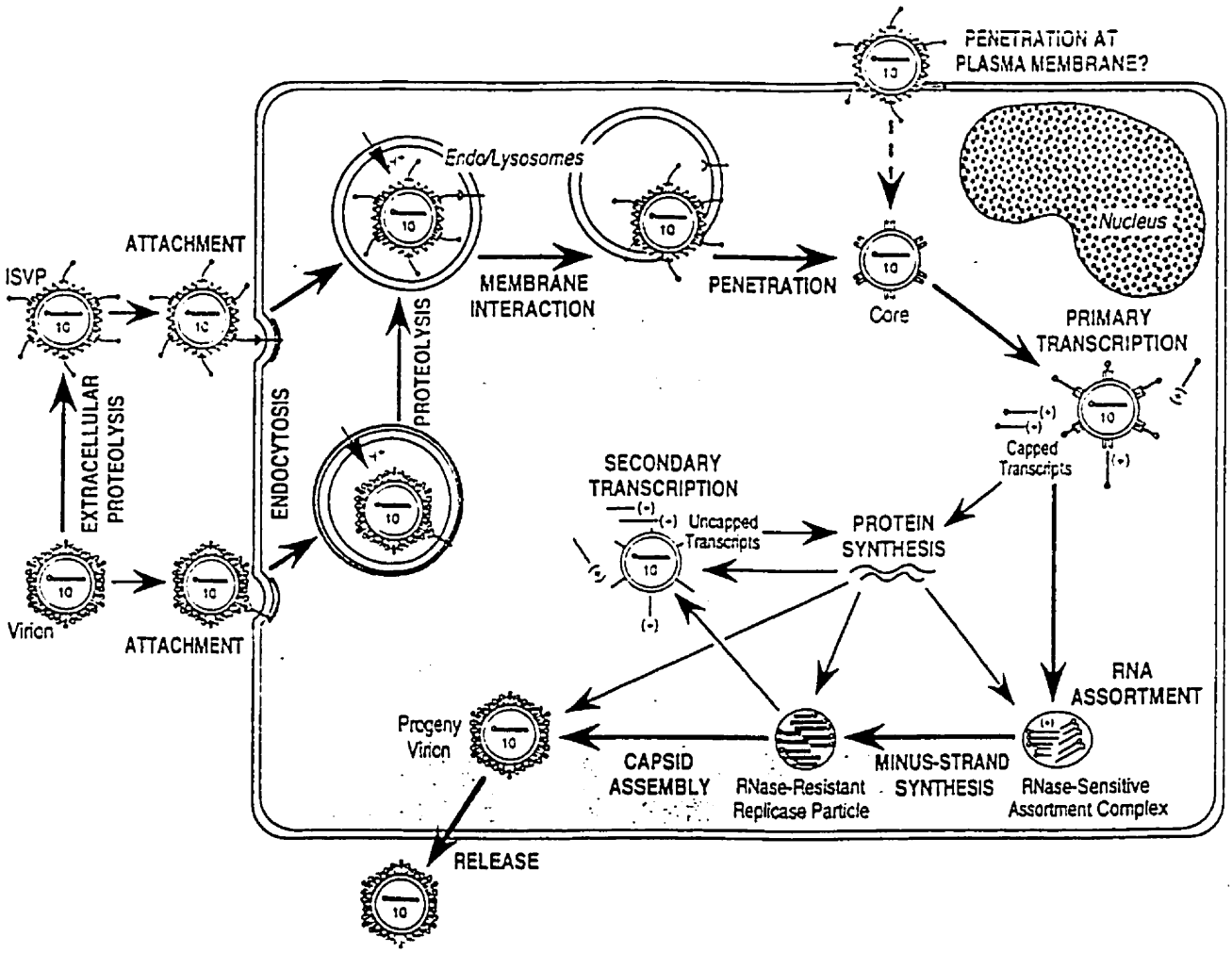
PENETRATION AT PLASMA MEMBRANE?
Endo/Lysosomes
Nucleus
ATTACHMENT
ISVP
MEMBRANE INTERACTION
PENETRATION
Core
PRIMARY TRANSCRIPTION
Capped Transcripts
EXTRACELLULAR PROTEOLYSIS
ENDOCYTOSIS
PROTEOLYSIS
SECONDARY TRANSCRIPTION
Uncapped Transcripts
PROTEIN SYNTHESIS
Virion
ATTACHMENT
RNA ASSORTMENT
Progeny Virion
CAPSID ASSEMBLY
RNase-Resistant Replicase Particle
MINUS-STRAND SYNTHESIS
RNase-Sensitive Assortment Complex
RELEASE

cases with hemorrhaging and variable inflammatory responses (Spriggs et al., 1983; Tyler and Fields, 1996; Figure 2). The striate cortex, cingulate gyrus and limbic system including Ammon's horn, septal nuclei, mammillary bodies were the areas found to be maximally involved (Spriggs et al., 1983; Tyler and Fields, 1996). The thalamus, basal ganglia, cerebellum, upper brain stem were also found to be frequently involved (Spriggs et al., 1983; Tyler and Fields, 1996). These effects have been found to be dependent on the route of viral infection. Infection by intracerebral or subcutaneous injection, or oral administration into the respiratory tract resulted in the aforementioned effects for both serotypes, however oral administration produced the effects associated with serotype 1 Lang infection but did not result in the effects seen with type 3 Dearing infection (Rubin and Fields, 1980).

In suckling mice, infection with any of the three serotypes causes myocarditis, alveolar hemorrhage and pulmonary edema, pancreatic and salivary gland injury, as well as hepatocellular damage thought to be responsible for the oily hair/runting syndrome often found in infected newborn mice (Stanley and Leak, 1963). Nervous system penetration of the three prototype strains of reovirus has also been studied in suckling mice (Flamand et al., 1991). Type 3 Dearing was found to enter both motor and sensory neurons in the dorsal root ganglia and spinal cord. Infection of neurons was clearly detectable by immunohistochemical staining 19 hours post-infection (Flamand et al., 1991). Several hundred motor and sensory neurons and interneurons were infected by day 4 as infection included large areas of the brain stem and brain (Flamand et al., 1991). Reovirus type 2 Jones also entered neurons. Reovirus type 1 Lang followed neuronal pathways as well as being disseminated in the bloodstream (Flamand et al., 1991). The titer of type 1 Lang increased in the bloodstream over time. This was not observed following infection with either of the other two strains (Flamand et al., 1991).

Infection of adult severe combined immunodeficient (SCID) mice via oral administration with either serotype 1 Lang or serotype 3 Dearing resulted in symptomatic disease and death in 4 – 6 weeks (Georgi et al., 1990). After primary replication in intestinal tissue however some SCID mice live more than 100 days as they develop a chronic infection

Figure 1.2. (a to e) Diagrams of coronal brain sections extending from rostral (*top left*) to caudal (*bottom right*) areas of the brain showing the location of virus-induced lesions in neonatal mice infected intracerebrally with either T3D or T3D variants with amino acid substitutions in the σ1 cell attachment protein. Black areas indicate regions of the brain in which T3D virus as well as the variant viruses induced lesions; dotted areas show regions in which only the T3D virus caused necrosis. [ac, anterior colliculus; c, cingulum; cn, caudate nucleus; dg, dentate gyrus; dnh, dorsomedial nucleus of the hypothalamus; h, hippocampus; lgb, lateral geniculate body; ltn, lateral thalamic nucleus; lv, lateral ventricle; mb, mammillary bodies; msn, medial septal nucleus; oc, occipital cortex; s, subiculum; sn, substantia nigra; stn, spinal trigeminal nucleus; tv, third ventricle; zi, zona incerta]. (f and g) Growth patterns of (f) the Dearing strain of reovirus type 3 and (g) the variant virus in various organs after intraperitoneal inoculation of virus. Virus growth in (•) brains, (Δ) spleens, and () liver was determined after injection of 10^7 PFUs of either virus. Mice were killed at each time point and the virus titers were determined by titration of organ homogenates on L929 cells. Each value being representative of three titrations (Spriggs et al., 1983; Tyler and Fields, 1996).

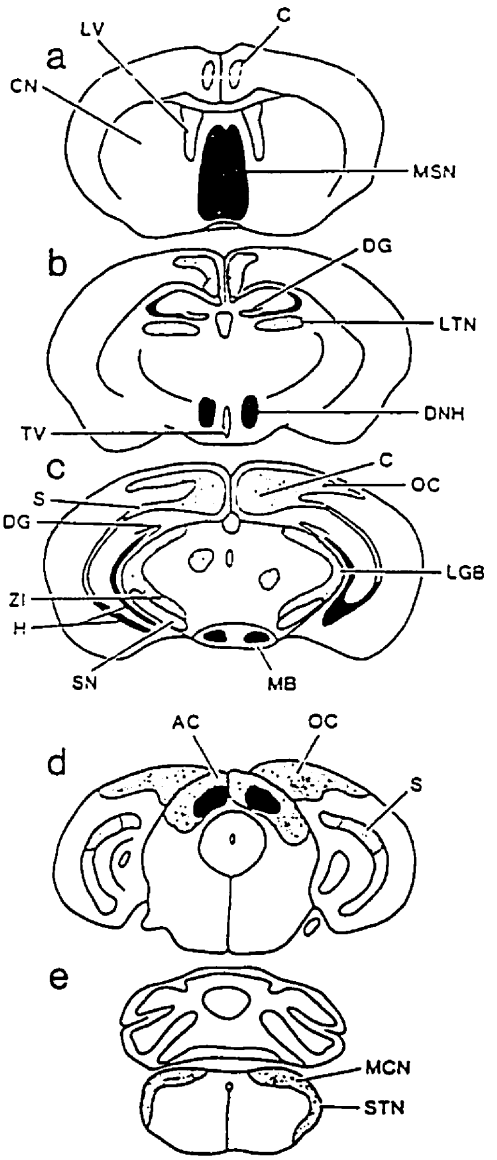
a
LV
C
CN
MSN
b
DG
LTN
DNH
TV
c
C
OC
S
DG
LGB
ZI
H
SN
MB
d
AC
OC
S
e
MCN
STN

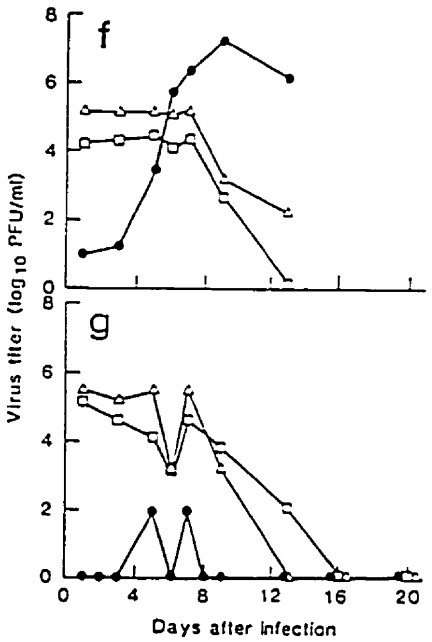
f
g
Virus titer (log10 PFU/ml)
0
2
4
6
8
0
4
8
12
16
20
Days after infection

that can spread systemically (Haller et al., 1995a). Such prolonged infections resulted in the selection of organ-specific variants chosen at different stages of reovirus pathogenesis as they were more efficient than their wild type reovirus type 3 counterpart (Haller et al., 1995b). A brain specific variant (T3DvBr) has been isolated (Haller et al., 1995b); as it grew to higher titers than wild type reovirus in SCID mouse brain following intraperitoneal inoculation, killed adult SCID mice faster that type 3 Dearing and grew well in neonatal NIH Swiss mouse brain tissue after intramuscular but not peroral infection (Haller et al., 1995b).

1.1.5. Molecular basis of reovirus oncolysis

Significant differences have been found to exist in the susceptibility of different cell types to reovirus suggesting that infection may be somehow linked to the transformed state of the cell. Certain virally and spontaneously transformed cell lines of murine origin were found susceptible to reovirus infection, whereas normal human and subhuman primate cells, primary mouse cells, normal rat kidney cells and baby hamster kidney cells were not (Hashiro et al., 1977). Furthermore, normal and SV40-transformed WI-38 cells also displayed differential sensitivities to reovirus, with cytopathology observed only in the transformed cells and not in normal cells (Duncan et al., 1978). Normal cells were infected by reovirus, as they both produced and released, virus but exhibited no detectable cytopathology (Duncan et al., 1978).

By using cells transformed with defined oncogenes, it was determined that reovirus usurps the cellular Ras signaling pathway for its replication (Strong et al., 1998). Mouse fibroblast NIH 3T3 cells found resistant to reovirus infection became susceptible following their transfection with the gene encoding EGFR (Strong et al., 1993) or with the v-*erbB* oncogene (Strong and Lee, 1996). Transformation of the reovirus-resistant NIH 3T3 cells with activated Sos or Ras also resulted in enhanced viral infection (Strong et al., 1998). These findings proved to be indicative of a usurpation of the virus of activated host cellular pathways involving Ras or a downstream element. Activated Ras

Figure 1.3. The molecular basis of reovirus oncolysis: usurpation of the host cell Ras signaling pathway. For both untransformed (reovirus resistant) and EGFR-, Sos-, or Ras-transformed (reovirus susceptible) cells, virus binding, internalization, uncoating and early transcription of viral genes all proceed normally. In the case of untransformed cells, secondary structures on early viral transcripts inevitably trigger the phosphorylation of PKR, thereby activating it, leading to the phosphorylation of the translation initiation factor eIF-2α, hence the inhibition of viral gene translation. In the case of EGFR-, Sos- or Ras-transformed cells, the PKR phosphorylation step is prevented or reversed by Ras or one of its downstream elements, thereby allowing viral gene translation to ensue. The action of Ras (or a downstream element) in promoting viral gene translation (and hence reovirus infection) in the untransformed cells can be mimicked by deletion of the *Pkr* gene or by blocking PKR phosphorylation with 2-aminopurine (2-AP) (Strong et al., 1998).

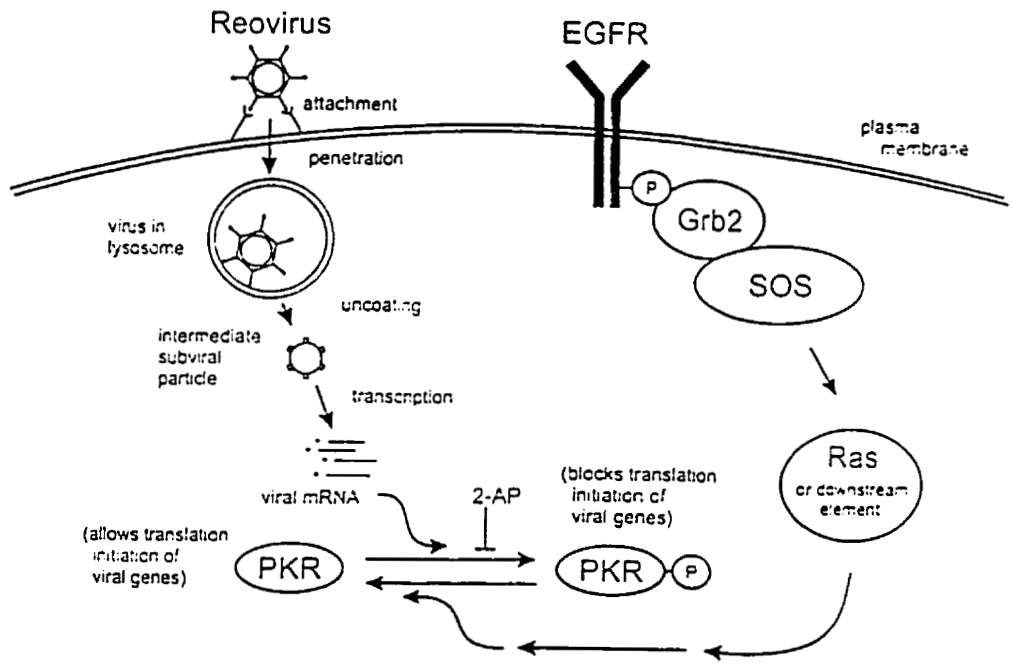
Reovirus
EGFR
attachment
penetration
plasma membrane
virus in lysosome
uncoating
intermediate subviral particle
transcription
viral mRNA
2-AP
(blocks translation initiation of viral genes)
(allows translation initiation of viral genes)
PKR
PKR
P
P
Grb2
SOS
Ras
or downstream element

(or an activated element of the Ras pathway) presumably inhibits (or reverses) double-stranded RNA-activated protein kinase (PKR) activation, thereby allowing viral protein synthesis and a productive infection to occur (Strong et al., 1998; Figure 3). PKR expression can be induced by IFN and the kinase activity is stimulated by low concentrations of dsRNA (DeHaro et al., 1996; Hovanessian, 1989). The reovirus s1 mRNA (mRNA for σ1 protein) has been found to activate PKR (Clemens and Elia, 1997). Reovirus protein σ3 (outer shell protein) has also been found to bind dsRNA and thereby stimulate translation by blocking PKR activation (Yue and Shatkin, 1997).

1.1.6. Other Oncolytic Viruses

Reovirus belongs to a growing family of viruses, both genetically altered and those that are unmodified, that have a propensity to replicate in transformed cells. This family includes both DNA and RNA viruses, which will be discussed separately as a matter of simplicity.

DNA viruses have evolved a variety of replication strategies to ensure their survival. The encoding of their own replication apparatus is one such strategy and the herpes virus is an example of viruses that employs this strategy. In addition to encoding a number of viral proteins that are directly involved in viral DNA replication (Tyler and Fields, 1996), HSV encodes three enzymes involved in the providing the virus with nucleoside triphosphate precursors for viral replication; ribonucleoside reductase, thymidine kinase, and dUTPase. As HSV exhibits its natural tropism to mitotically inactive neurons, a population of cells in which there is a low basal level of DNA precursors and DNA replication proteins, the virus has evolved to encode these proteins to allow efficient HSV replication in a environment that would otherwise not support viral growth.

A second strategy used by DNA viruses to ensure effective replication is to induce S-phase progression of the cell cycle (DNA synthesis), which is crucial if the virus depends exclusively on the host's replication apparatus for its own replication. This is of great importance since the DNA replication machinery could be limiting in quiescent cells. An

important example of this type of strategy is that employed by the human adenovirus that encodes three viral proteins to induce entry into S-phase. The E1A protein binds to the tumor suppressor, pRb, and disrupts the interaction between it and the transcription factor E2F (Tyler and Fields, 1996). E2F once released, activates genes required for cell cycle progression into S-phase. Moreover, adenovirus also encodes E1B-55Kd and -19Kd, involved in inactivating the G1 block that is imposed by host's p53 protein. In many viral infections, including adenovirus, p53 is up-regulated as a result of viral infection and resulting in cell cycle arrest and apoptosis. To prevent this, E1B 55Kd binds to, and inactivates, p53. For its part, E1A 19Kd, prevents the host cell from becoming apoptotic. Together, these proteins create a cellular environment that is optimal for adenovirus replication.

Understanding the replication requirements of these viruses in their normal cellular targets allows one to hypothesize how deletion of specific viral genes could compromise the ability of these cells to replicate in their normal host population. One would expect that in the case of HSV, deletion of any of the enzymes responsible for the creation of the nucleoside precursors would ultimately prevent HSV from replicating in quiescent neuronal cells where these precursors are limiting. Would these genes be required however, if these precursors were not limiting, in a population of rapidly dividing or tumorogenic neurons? Based on this premise, Martuza and co-workers, were able to demonstrate that thymidine kinase deficient HSV-1 was able to replicate in malignant gliomas but not surrounding tissue (Martuza, 1991).

More recently, Bischoff and co-workers have demonstrated the successful use of an E1B gene-attenuated adenovirus for the treatment of tumors lacking a functional p53 but this virus is apparently unable to replicate in normal cells (Bischoff, 1996; Heise, 1997). It would appear that because this virus is attenuated in the 55Kd portion of the E1B gene, wild type p53 is not blocked by this viral gene product. In cells lacking a functional p53, the need for E1B 55Kd becomes redundant, and therefore, this virus (designated ONYX-015) is able to replicate in these tumor cells. By this rationale then, it would seem possible that many DNA viruses that target either pRb or p53 for their replication could

potentially all act as oncolytic agents in tumors in which either pRb or p53 function is aberrant. A number of groups are already betting on this and an E1A attenuated adenovirus is being investigated as a means of treating retinoblastoma tumors (Heise, 1997). Whether, or not human papillomavirus (HPV) which targets p53 degradation with the viral product E6, or SV40 T antigen (TAg) which functions like adenovirus E1B will ever become useful strategies in cancer therapies, has yet to be seen.

Reovirus is not the only RNA virus that exhibits an oncolytic potential, although it is by far the best characterized. An additional RNA virus that exhibits a preference for replication in tumor cells is the Newcastle disease virus (NDV). NDV is a paramyxovirus of chickens. It has been demonstrated to have preferential replication in tumor cells that have an activated N-ras pathway (Lorence, 1994). Whether NDV uses a similar strategy to reovirus in promoting its oncolytic nature is at this time unknown. The observed specificity of reovirus to replicate only in those tumorigenic cells that possess activated Ras, combined with the lack of pathogenicity of the virus raises the interesting possibility that it could act as an oncolytic agent. The remainder if this dissertation will address the efficacy of reovirus as a glioma therapeutic.

1.2. MALIGNANT GLIOMAS

1.2.1. Classification

Primary brain tumors arise from cells of the CNS or its coverings. They are classified as being epithelial if they originate from neural, glial or neuroglial cells. In adults, neuroepithelial tumors account for 50-60% of primary intracranial tumors. (reviewed by Tatter and Harsh, 1998). The relative incidence of various neuroepithelial tumor types are as follows: glioblastoma multiformes, 50%; anaplastic astrocytomas, 30%; oligodendrogliomas, 6%; nonanaplastic astrocytomas, 5%; ependymal cell tumors,4%; medulloblastomas, 2%; and nerve cell, neuroblastomas, pineal cell tumors, subependymal giant cell astrocytomas, pilocytic astrocytomas, and choroid plexus tumors, each less than 1% (Tatter and Harsh, 1998). The most common types of non-neuroepithelial brain tumors are meningiomas followed by schwannomas, which account for approximately 20% of brain tumors. Secondary or metastatic brain tumors result from the metastasis of a cancer arising from tissues outside of the CNS (e.g. lung) as well as those tumors arising in nearby tissues that directly invade the brain (Tatter and Harsh, 1998).

Malignant gliomas comprise the majority of primary brain tumors (Forsyth and Cairncross, 1996; Scott et al., 1999). These tumors may arise from brain parenchyma without apparent antecedent, or may result from malignant transformation of less anaplastic astrocytomas, mixed tumors, oligodendrogliomas, or ependymomas (Tatter and Harsh, 1998). Glioblastomas are considered the malignant extreme on the continuum of astrocytic tumors, as the cellular differentiation that occurs in some gliomas is usually astrocytic and because many gliomas result from the malignant degeneration of pre-existing astrocytic tumors (Tatter and Harsh, 1998). Brain tumors are the second leading cause of cancer death in children.

Malignant gliomas represent a major therapeutic challenge, as they are poorly circumscribed, highly aggressive and are typically refractory to surgery, radiotherapy,

and chemotherapy. The median survival for the most aggressive of these gliomas (GBMs) is only 1 year and < 2% survive 3 years or longer (Scott et al., 1999), despite recent advances in neurosurgical techniques and radiation therapy. Given their dismal prognosis, there is strong rationale for examining the efficacy of novel therapeutic strategies as a means for enhancing disease control.

1.2.2. Molecular characteristics of malignant gliomas

Molecular studies have identified some of the genetic changes that underlie the pathological differences among astrocytic tumors. The progression of astrocytomas is slowly evolving process that involves both tumor suppressor genes and oncogenes (Figure 4; Table 2). Mutations have been identified in the p53 tumor suppressor gene on chromosome 17p in low grade astrocytomas, suggesting that this may be an early pathological event (von Deimling et al., 1992). Loss of the entire or parts of chromosome 10 is exclusively found in GBMs and not in low grade astrocytomas (Pershouse et al., 1993; James and Collins, 1992; James et al., 1988). PTEN/MMAC, a dual specific phosphotase identified as a tumor suppressor gene on chromosome 10, has also been associated with GBMs (Li and Sun, 1997; Li et al., 1997; Steck et al., 1997). The multiple tumor suppressor (MTS1) gene, encoding for the cell cycle inhibitor p16, may also be relevant in malignant astrocytoma progression (Kamb et al., 1994; Noborl et al., 1994) as may the loss of heterozygosity on 19q (Rubio et al., 1994).

The proto-oncogene c-*erbB* which encodes for the epidermal growth factor receptor (EGFR) is located on chromosome 7 and is amplified in about 50% of GBMs (Libermann and Razon, 1984; Libermann et al., 1985). In those GBMs with amplified EGFR, 25-40% express both normal (170 kDa) and a truncated EGFR (140^{EGFR}) which is unable to bind EGF or TGF-α (Steck et al., 1988; Ekstrand et al., 1992; Ekstrand et al., 1994). Other proto-oncogenes frequently amplified or mutated in gliomas would include: MDM2 (Reifenberger et al., 1993), and platelet-derived growth factor receptor (PDGF-R) (Liang et al., 1994). Less frequently seen is the activation of proto-oncogenes including C-*myc*, N-*myc* and N-*ras* (Liang et al., 1994).

TABLE 2. GENETIC ALTERATIONS IN PRIMARY HUMAN CNS TUMORS

Tumor Type	Probe	Aberration
Astrocytoma	c-erbB (EGFR)	A
	c-myc	EE
	v-fos	EE
	v-sis	EE
	p53	mutation
Anaplastic Astrocytoma	c-erbB (EGFR)	A, RA
	N-myc	A
	c-sis (PDGF)	EE
	p53	mutation
Glioblastoma multiforme	c-erbB (EGFR)	A, RA, EE
	gli	A, EE
	N-myc	A, EE
	v-myc	EE
	v-sis	A, EE
	c-sis (PDGF)	EE
	v-fos	EE
	N-ras	A, EE
	Ha-ras	rare alleles
	c-mos	rare alleles
	Rb gene	deletion
	p53	point mutation
Oligodendroglioma	c-erbB (EGFR)	A, RA
	Ha-ras	rare alleles
	c-mos	rare alleles
Medulloblastoma	c-erbB (EGFR)	A
	N-myc	A, RA
	c-myc	A, EE
	v-myc	EE
	N-ras	point mutation
	p53 gene	mutation
Meningioma	c-sis (PDGF)	EE
	c-myc	A
	c-fos	EE
	N-myc	A, RA
	Ha-ras	rare alleles
	c-mos	rare alleles

Abbreviations: A = gene amplification; RA = gene rearrangement; EE = enhanced gene expression

(Gonzales, 1995)

Figure 1.4. The molecular pathogenesis of human astrocytomas. The progression from a grade III (anaplastic astrocytoma) to a highly-malignant glioblastoma multiforme is characterized by the loss of PTEN/MMAC and other putative tumor suppressor genes on chromosome 10 and amplification of the EGFR gene. The question mark (?) refers to those patients who present at *initio* with glioblastoma multiforme; whether these tumors progress through each step of this progression (either very rapidly or in a subclinical state) or skip various stages is not currently known (Guha, 1998).

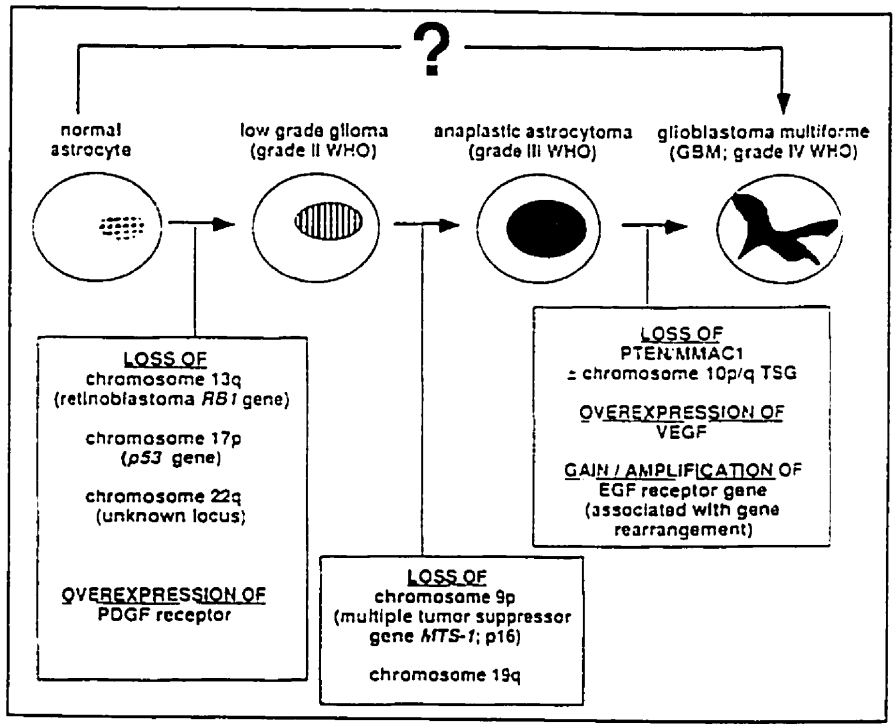
?
normal astrocyte
low grade glioma (grade II WHO)
anaplastic astrocytoma (grade III WHO)
glioblastoma multiforme (GBM; grade IV WHO)
LOSS OF
chromosome 13q
(retinoblastoma RB1 gene)
chromosome 17p
(p53 gene)
chromosome 22q
(unknown locus)
OVEREXPRESSION OF
PDGF receptor
LOSS OF
chromosome 9p
(multiple tumor suppressor gene MTS-1; p16)
chromosome 19q
LOSS OF
PTEN/MMAC1
± chromosome 10p/q TSG
OVEREXPRESSION OF
VEGF
GAIN / AMPLIFICATION OF
EGF receptor gene
(associated with gene rearrangement)

1.3. Rationale for using Reovirus as a Brain Tumor Therapy

Given the dismal prognosis of GBMs, there is strong rationale for examining the efficacy of novel therapeutic strategies as a means for enhancing disease control. Since Ras-activated pathways are present in the majority of malignant gliomas we were prompted to examine the potential usefulness of reovirus treatment for this form of cancer. In contrast to systemic cancers, oncogenic *ras* mutations are infrequent in gliomas. PDGF- and EGF-receptors and probably other receptor tyrosine kinases expressed by human malignant gliomas are capable of activating the Ras signaling pathway (Guha, 1998). EGFR is more commonly expressed with increasing grade of malignancy (Libermann et al., 1985; Libermann et al., 1984; Helseth et al., 1988; Gerosa et al., 1989; Hurtt et al., 1992). The PDGF receptor-α is over-expressed in approximately 25% of glioblastoma multiforme specimens (Guha, 1992; Guha et al., 1995).

Secondly, these are highly invasive tumors. Their invasive tendrils extend far beyond the main tumor mass rendering them surgically incurable and isolated tumor cells are commonly found several centimeters from the main mass. Reovirus may prove to be an effective glioma therapy as it targets and kills both local and remote tumor cells.

1.4. Hypothesis

It is hypothesized that reovirus will cause the oncolysis of cell lines derived from specimens from brain tumor patients *ex vivo* as well as established gliomas cell lines. It is further hypothesized that reovirus will cause regression, and possibly cure tumors in animal models of malignant gliomas.

1.5. Specific Aims

1) To determine whether reovirus can infect and kill human malignant glioma derived cell lines *in vitro* and if this correlates with constitutive Ras/MAPK signaling.
2) To identify brain tumors (from biopsy samples) susceptible to reovirus oncolysis *ex vivo*.
3) To determine the effects of reovirus on experimental malignant gliomas induced in both immunocompromised and immune-competent animal models.

CHAPTER 2: MATERIALS AND METHODS

2.1. Cell lines

U87, U87lacZ, U118, U178, U251N, U251lacZ, U343, U373, U563, RG2, 9L, 9LlacZ, A172, SF162, SF188, TE671, HTB185, HTB187, C6, C6lacZ, and SNB19 cell lines were originally obtained from the ATCC and were grown in Dulbecco's modified Eagle medium (DMEM; Gibco-BRL) containing 10% (volume/volume) fetal bovine serum (FBS). Cells were passaged when they reached approximately 80% confluence, harvested by trypsin treatment and replated in DMEM-F12/10% FBS. Cells were maintained in a humidified incubator at 37°C in a 95% air/5% carbon dioxide atmosphere (CO_2). Cell lines were routinely tested for mycoplasma contamination.

2.1.1. Cell lines from tumor specimens

A number of low passage, human glioma cell strains were established at our institution from tumor specimens that were transported directly from the operating room to the laboratory in DMEM. The specimen was split in half, part of it being fixed in formalin (to confirm the identity of the growing cells) and the other part was placed in DMEM with 20% FBS. The tissue was then washed in DMEM, cut into pieces ~1-2 mm in diameter, sent through a cell screen (removed connective tissue and vessels) and then further disaggregated by sequential 20 min exposures to trypsin (0.5%) and EDTA (0.53 mM) in Dulbecco's PBS. Cells were then suspended in FBS, pelleted (200 x g for 8 min), resuspended in DMEM/F12 + 20% FBS and cultured in 150 cm^2 flasks. Cultures became confluent 3-4 weeks later and were then harvested with trypsin-EDTA. Cells were then replated for infectibility and MAPK assays at 10^4 cells/well in DMEM/F12 (+ 5% FBS + L-glutamine: 300 µl/well) and on glass coverslips. The 9 glioma cell lines were derived from 4 GBMs, 3 anaplastic astrocytomas, 1 non-anaplastic astrocytoma and 1 oligodendroglioma. We also cultured 7 meningiomas (1 spinal cord meningioma) and 1 metastatic carcinoma (metastasis from the lung). Our Conjoint Medical Ethics Committee approved this study. A neuropathologist confirmed the histopatholgical diagnosis.

2.2. Virus

The Dearing strain of reovirus serotype 3 used in these studies was propagated in suspension cultures of L cells and purified according to Smith et al. (1969) with the exception that β-mercaptoethanol (β-ME) was omitted from the extraction buffer.

2.2.1. Plaque assay

Virus was titrated on L929 cell monolayers by modification of the procedure of Shaw and Cox (1973). Approximately 10^6 L929 cells were added to 6-well plates and after 4-5 hrs of incubation at 37°C, the medium was removed and 0.2 ml of each virus dilution was added. The L929 cells were then incubated for 45-60 mins at 37°C in an atmosphere of 5% CO_2 in air. Cultures were "flicked" every 5 minutes to ensure that the L929 cells remained wet. 2.5 mLs of JMEM containing 5% FBS and 1% agar was then added to each well and allowed to solidify. The cultures were then incubated at 37°C in 5% CO_2 in air for 72 hrs. A second overlay containing neutral red was then added and incubation was continued for 24 hrs, after which plaques were counted.

2.2.2. Infection of cells and quantification of virus

Confluent monolayers of cells grown in 24-well plates were infected with reovirus at an estimated multiplicity of infection (MOI) of 10 PFU/cell. After 1 hr incubation at 37°C, the monolayers were washed with warm JMEM + 5% FBS, and then incubated in the same medium. At various times post-infection, a mixture of NP-40 and sodium deoxycholate was added directly to the medium on the infected monolayers to final concentrations of 1% and 0.5% respectively. The lysates were then harvested and virus yields were determined by plaque titration on L929 cells.

2.2.3. Cell killing

Cells were grown to approximately 80% confluency and then exposed to reovirus (MOI = 10 PFU/cell). The extent of cell killing upon infection of different cell lines was estimated by the percentage of residual cells excluding trypan blue. The cytopathic effects of viral infection were visualized by light microscopy (Olympus IX70). Cells were photographed 48 hrs following infection.

2.2.4. Determination of viral titer in brain tissues

Brain tissue flash frozen in liquid nitrogen at the time of sacrifice was stored at -80°C until use. Tissues were suspended in 0.5 mL of JMEM, manually homogenized and then sonicated briefly with a microtip probe (Ultrasonic XL sonicator) at setting 2. Homogenization mixture was then repeatedly frozen and thawed in CO_2 and ethanol followed by centrifugation at 10000 rpm for 5 mins. Serial 10-fold dilutions were then made in JMEM prior to inoculation of L929 cell monolayers in six-well plates (10^6 cells per well). Duplicate wells for each of three dilutions were inoculated, and plaque assays were performed as described previously.

2.3. Animals

Five to eight week old male/female SCID NOD mice were purchased from Cross Canada Institute (CCI). Five to eight week old male/female nude mice were purchased from Charles River Canada. Male/female Fischer 344 rats (Harlan Sprague Dawley) weighing 180-200 g (8-10 weeks of age) were used in these studies. The animals were housed in groups of 2-6 in a vivarium maintained on a 12-hr light/dark schedule with a temperature of 22 ± 1°C and a relative humidity of 50 ± 5%. Food and water were available ad libitum to all study animals. All procedures were reviewed and approved by The University of Calgary Animal Care Committee.

2.3.1. *In vivo* studies in a subcutaneous (s.c.) tumor model in SCID NOD mice

Actively growing U87 or U251N cells were harvested, washed, and resuspended in sterile PBS at a density of 2 x 10^7 cells/ml. 2.0 x 10^6 cells in 100 µl sterile PBS were injected s.c. at a site overlying the hind flank of male SCID NOD mice. Implanted tumors were allowed to grow for 2-3 weeks until palpable tumors of 0.5 x 0.5 cm were obtained. They were then given a single intratumoral (i.t.) injection of 1.0 x 10^7 PFUs of either live or dead (UV-inactivated) reovirus in 20 µl sterile PBS. Tumor size (length x width) was measured twice weekly for a period of two to four weeks. All animals were sacrificed when either the control group of mice (i.e., those receiving the dead virus) showed severe morbidity due to excess tumor burden or the live-virus treated mice showed 20% body weight loss or hind limb necrosis.

2.3.2. *In vivo* studies in a s.c. tumor model in Fischer 344 rats

6-8 week old Fischer 344 male rats were injected with 10^6 cells in a 100 µl volume in the flank as described above. Implanted tumors were allowed to grow until they measured 1.0 x 1.0 cm; animals were then given a single i.t. injection of 10^9 PFUs of either live or dead reovirus every day for 1 week and then every second day for three weeks. Tumor size (length x width) was measured twice weekly for a period of two to four weeks. All animals were sacrificed when the control group of mice (i.e., those receiving the UV-inactivated virus) lost 25% of their body weight, or had impaired ambulation due to excess tumor burden. At the time of sacrifice, residual tumor masses of live virus treated rats were pierced with a pin and the contained fluid drained into a conical tube to determine whether the "tumor area" measured was representative of "true" tumor. The contents of the tube were then spun, supernatant discarded and the remainders frozen in OCT for frozen sectioning.

To determine if pre-existing antibodies to reovirus would abrogate the oncolytic effects of reovirus. Reovirus antibodies were raised in Fischer rats following challenge with an

intramuscular injection of reovirus (10^7 PFUs). To ensure that antibodies were in fact raised, an agglutination inhibition assay was performed.

2.3.3. *In vivo* studies in an intracranial glioma model

The ability of reovirus to cause regression of human glioma cells xenotransplanted into the right cerebral hemisphere was tested in SCID NOD mice. Actively growing U87lacZ or U251N cells were harvested, washed, and resuspended in sterile PBS. 2.0 x 10^6 cells in 2 µl of PBS were injected intracerebrally. A midline scalp incision was made, and a 0.5-mm burr hole was made 1.5-2 mm to the right of the midline and 0.5-1 mm posterior to the coronal suture. Tumor cells were resuspended in sterile PBS and stereotactically injected using a 5-µl Hamilton syringe with a 30-gauge needle mounted on a KOPF stereotactic apparatus. The needle was inserted vertically through the burr hole to a depth of 3 mm. Sixty seconds following injection, the needle was slowly withdrawn and then the incision sutured. Implanted tumors were allowed to grow for 14 days at which time a single intratumoral injection of 10^7 PFUs of either live or dead (UV-inactivated virus) in 2 µl of PBS was administered. All mice were anesthetized by intraperitoneal (i.p.) administration [ketamine (8.5) plus xylazine (1.5)- MTC Pharmaceuticals, Cambridge Ontario]. Animals were euthanized when they lost 20% of their body weight or had difficulty feeding or ambulating. Animal studies were conducted in accordance with guidelines for animal use and care established by the University of Calgary Animal Resource Program.

2.3.4. Replication of reovirus in an intracranial model in immunocompetent rats

To determine if reovirus produces viral encephalitis/cerebral edema, live and actively replicating virus (10^9 PFUs) was injected stereotactically into the right cerebral hemisphere. Fischer rats were sacrificed at different time points (0 hr, 1 hr, 12 hrs, 24 hrs, 48 hrs, and 72 hrs, 1 month and 3 months) following initial infection, and brain tissues were harvested, homogenized, and the lytic capacity of the supernatant was then assayed on L929 cells. Brains from mice receiving live reovirus were fixed and stained (H&E) to determine the

presence of inflammation, edema and brain infection adjacent to and remote from the site of virus administration.

2.3.5. Intracranial cannulation

Female Fischer 344 rats were anaesthetized and placed in a stereotactic unit. A 2 cm midline scalp incision was made, and 4 0.5-mm burr holes were made; one 1.5-2 mm to the right of the midline and 0.5-1 mm posterior to the coronal suture for cannula and three holes around this sight for the placement of screws. The cannula was then lowered into the skull to a depth of 3.5 mm, screws screwed in and dental cement was used to keep the cannula in place. Using wound staples, the incision was sutured. At experiment termination, rats were euthanized by cardiac administration of 1 c.c. of euthanyl [MTC Pharmaceuticals; Cambridge, Ontario].

2.3.6. Treatment of a syngeneic glioma model using a cannula delivery system

The ability of reovirus to cause regression of rodent 9L glioma cells xenotransplanted into the right cerebral hemisphere was tested in female Fischer 344 rats. Actively growing 9L cells were harvested, washed, and resuspended in sterile PBS. 5.0×10^4 cells in 2 µl of PBS were injected intracerebrally through a cannula that was previously implanted. The tumor cells were allowed to grow for 2-4 days at which time injections of either live or dead virus in PBS were administered (every 48 hrs until animals became moribund).

2.3.7. Blood collection and quantitation of virus

Blood was collected by cardiac puncture at the time of animal sacrifice and viral plaque assays were performed to determine the amount of circulating virus.

2.4. Immunofluorescent analysis of reovirus infection

For the immunofluorescent studies, cells were grown on coverslips, and infected with reovirus at a MOI of ~10 PFU/cell, or mock-infected. At 48 hrs post-infection, cells were fixed in an ethanol/acetic acid (20/1) mixture for 5 mins and then sequentially rehydrated by sequential washes in 75, 50 and 25% ethanol, followed by four washes with phosphate-buffered saline (PBS). For paraffin-embedded tumor sections, slides were treated with xylene and again subsequently rehydrated by sequential washes in 75%, 50% and 25% ethanol followed by 4 washes with PBS. The fixed and rehydrated sections/cells were then exposed to the primary antibody (rabbit polyclonal anti-reovirus type 3 serum diluted 1/100 in PBS) for 2 hrs at room temperature. Following three washes with PBS, the cells were exposed to the secondary antibody (goat anti-rabbit IgG [whole molecule] fluorescein isothiocyanate (FITC) conjugate diluted 1/100 in PBS containing 10% goat serum and 0.005% Evan's Blue counterstain) for 1 hr at room temperature. Finally, the fixed and treated cells were washed 3 more times with PBS, followed by 1 wash with double-distilled water, dried and mounted on slides in 90% glycerol containing 0.1% phenylenediamine, and viewed with a Zeiss Axiophot microscope mounted with a Carl Zeiss camera.

2.5. Detection of mitogen activated protein (MAP) kinase (ERK) assay

The 'PhosphoPlus' p44/42 MAP kinase (Thr202/Tyr204) Antibody kit (New England Biolabs) was used for the detection of MAP kinase in cell lysates according to the manufacturer's instructions. Briefly, subconfluent monolayer cultures were lysed with the recommended SDS-containing sample buffer, and subjected to SDS-PAGE, followed by electroblotting onto nitrocellulose paper. The membrane was then probed with the primary antibody (anti-total MAPK or anti-phospho-MAPK), followed by the horseradish peroxidase (HRP)-conjugated secondary antibody as described in the manufacturer's instruction manual.

2.6. Radiolabelling of reovirus-infected cells and preparation of lysates

Confluent monolayers of malignant glioma cell lines were infected with reovirus (MOI ~10 PFU/cell). At 46-48 hrs post-infection, the medium was replaced with methionine-free DMEM containing 10% dialyzed FBS and 0.1 mCi/ml of [^{35}S]-methionine. After further incubation for 2-4 hrs at 37°C, the cells were washed in PBS and lysed in the same buffer containing 1% Triton X-100, 0.5% sodium deoxycholate and 1 mM EDTA. The nuclei were then removed by low-speed centrifugation and the supernatants were stored at -80°C until use.

2.6.1. Immunoprecipitation and SDS-PAGE analysis

Immunoprecipitation of ^{35}S-labelled reovirus-infected cell lysates with anti-reovirus serotype 3 serum was carried out as previously described (Lee et al., 1981). Immunoprecipitates were analyzed by discontinuous SDS-PAGE according to the protocol of Laemmli (1970).

CHAPTER 3: RESULTS

3.1. Reovirus is effective *in vitro* at killing glioma cell lines.

We analyzed the susceptibility of 23 established glioma cell lines to reovirus. Following challenge with reovirus, the morphology of uninfected and infected cell lines was compared by indirect microscopy. Dramatic and widespread cell killing was seen in 19 (~80%) of 23 cell lines. A representation of the cytopathic effects of the virus on three glioma cell lines can be seen in Figure 3.1. After 48 hours of infection widespread cell death can be seen in U87, U251N and A172 cells treated with live reovirus (dead cells are rounded and non-adherent). Almost complete cell death is seen 72 hours following infection. In contrast, cells receiving either dead or no virus all remained healthy. U118 was the most poorly infectible cell line, as it was not killed with reovirus even at 72 hours post-infection. To ensure that the lysis of these cells was in fact due to viral replication, cells were fixed, processed and reacted with rabbit anti-reovirus antibody, followed by FITC-conjugated goat anti-rabbit IgG. Results (Figure 3.2) demonstrate that U87, U251N and A172 cells were very susceptible to infection 48 hours following reovirus exposure whereas U118 was poorly infectible. Replication of reovirus was confirmed further by the metabolic labeling of cells with [^{35}S]-methionine followed by SDS-PAGE analysis of virus specific proteins (Figure 3.3A *left panel*). Results clearly showed that 83% of the tested glioma cell lines (e.g. U87, U251N and A172, etc.) synthesized reovirus viral proteins (Table 3). The identities of viral bands were confirmed by immunoprecipitation of labeled proteins with polyclonal anti-reovirus antibodies (Figure 3.3A *right panel*). Reovirus replication however was restricted in U178, U118, U373, and SF188 (data not shown). MAPK was activated in 90% of the cell lines found to be susceptible to reovirus protein synthesis (Figure 3.3B and C). As expected no MAPK phosphorylation was found in the resistant lines U118 and U373. In contrast, SF126 and U343 cell lines were susceptible but showed no MAPK activation. These results suggest that a high percentage of brain cancers could potentially be treatable by viral therapy.

Figure 3.1. Effects of reovirus *in vitro* on established glioblastoma cells. Cytopathic effect. U87, U251N, A172 and U118 cells grown to 80% confluency were exposed to reovirus (MOI = 40 PFUs per cell). Following 48 hours of viral challenge, dramatic and wide spread cell killing is evident in the U87, U251N and A172 cell lines. Cells were photographed 48 and 72 hours following infection.

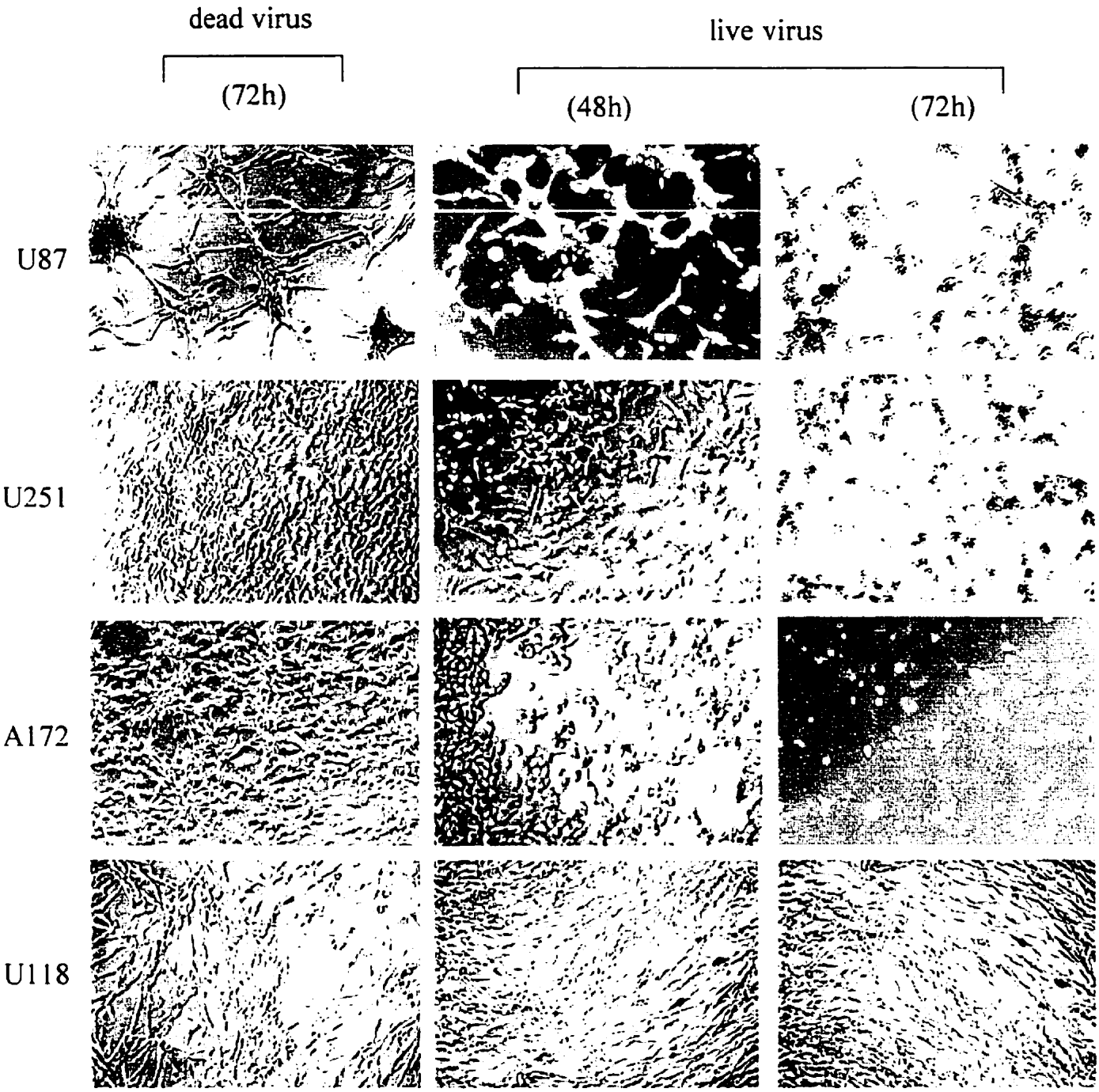
dead virus
(72h)
live virus
(48h)
(72h)
U87
U251
A172
U118

Figure 3.2. Immunofluorescent assay of viral proteins expressed in reovirus-infected U87, U251N, A172 and U118 cells. Cells were infected with reovirus at an estimated MOI of 10 PFUs per cell. At 48 post infection, cells were fixed, processed and reacted with rabbit anti-reovirus type 3 antibody and then with FITC-conjugated goat anti-rabbit immunoglobulin G (cells were counterstained with Evan's blue). Results demonstrate that U118 was poorly infectible whereas U87 and 9L cells were much more susceptible to infection. Magnification 200X for all pictures.

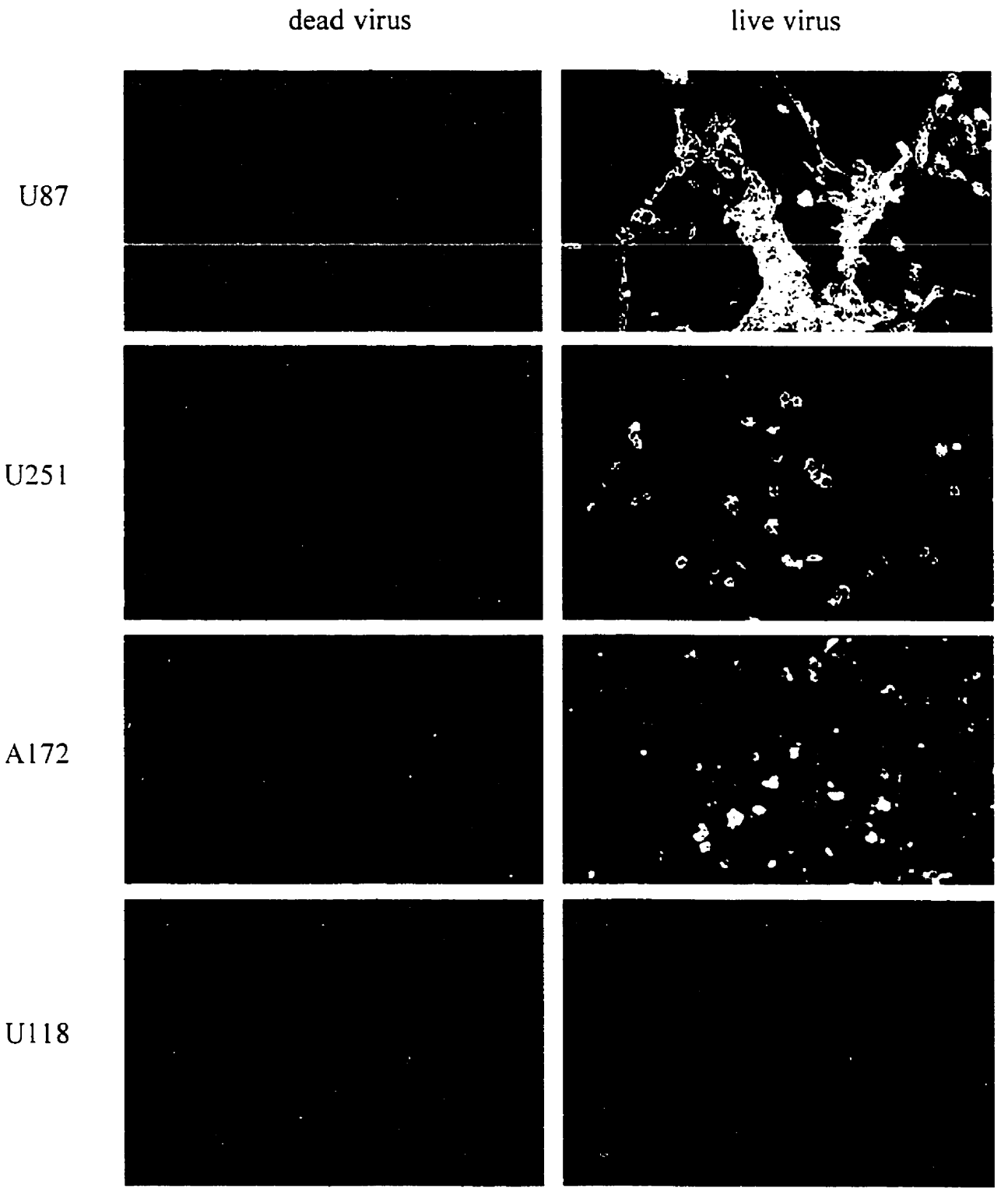
dead virus
live virus
U87
U251
A172
U118

Figure 3.3. (A) Reovirus protein synthesis in mock-infected and reovirus-infected U87, U251N, A172 and U118 cell lines. Monolayers were infected with reovirus at a multiplicity of infection (MOI) of 40 PFUs/cell. Cells were labeled with [^{35}S] - methionine from 42-48 hours after infection. Lysates were prepared and subsequently analyzed by SDS-PAGE (*right panel*; immunoprecipitated with a polyclonal anti-reovirus type 3 serum *left panel*). Reovirus proteins (3 size groups: λ, μ, and σ) are indicated on the right. Reovirus infection (as indicated by the presence of reovirus proteins λ, μ, and σ) is clearly evident in 3 of these 4 cell lines. A total of 23 glioma cell lines were tested for reovirus infection, 19 (83%) of which proved to be susceptible. [+ = infected; - = mock-infected] (B) Reovirus infectivity correlates with constitutive MAPK phosphorylation. The glioma cell lines U87, U251N, A172 and U118 were plated in a six well plate. Cells were either grown in the presence of 10% FBS or were serum starved (0.5% FBS) for a 48 hours. Monolayers were washed in PBS and cell lysates were prepared and subjected to SDS-PAGE. Following blotting onto nitrocellulose paper, samples were probed samples were probed with antibodies directed against phospho-MAPK. Phospho-MAPK levels were all standardized by total MAPK levels. MAPK assay shows phosphorylation in most cell lines that were found susceptible to infection (SF126 and U343 cell lines were found susceptible but showed no MAPK activation); no phosphorylation was seen in U118 or U373 (data not shown). Other cell lines found non-susceptible to infection as well as being negative for MAPK activation were U178 and SF188 (data not shown). (C) Total MAPK levels in glioma cell lines.

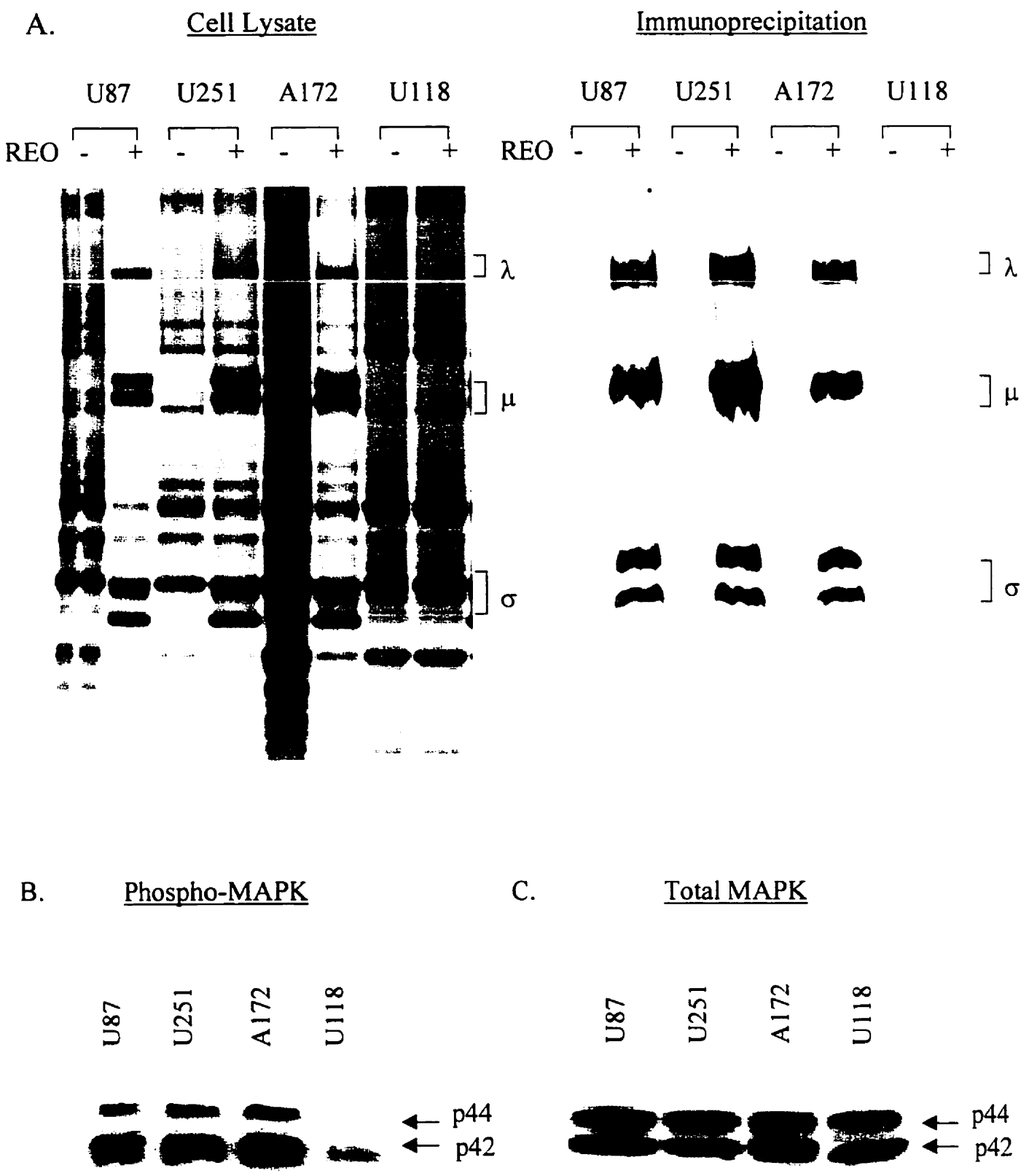
A.
Cell Lysate
Immunoprecipitation
U87
U251
A172
U118
REO
- + - + - + - +
λ
μ
σ
B.
Phospho-MAPK
C.
Total MAPK
U87
U251
A172
U118
p44
p42

TABLE 3: EFFECTS OF REOVIRUS *in vitro* ON ESTABLISHED GLIOMA CELL LINES.

	Susceptible	Non-susceptible
MAPK Phosphorylation	U87 U87lacZ U251N U251lacZ 9L 9LlacZ RG2 A172 TE671 HTB185 HTB187 U563 C6 C6lacZ SNB19 UC10 UC12 UC13 UC17 UC29 = 20	
No MAPK Phosphorylation	SF126 U343 = 2	U118 U373 U178 SF188 UC18 = 5

MAPK Phosphorylation/ Susceptible = 20/27 = 74% Total Susceptible = 82%
No MAPK Phosphorylation/ Non-susceptible = 2/27 = 7% Total Non-susceptible = 18%
No MAPK Phosphorylation/ Susceptible = 5/27 = 19%

* note: The ATCC believes that SNB19 and U343 are the same cell line. We have had these cell lines in the laboratory for over two years as they have been passaged a number of times but we have not actually ascertained whether or not they are the same. Given the discrepancy in MAPK phosphorylation status between these cell lines our results would suggest that the lines in our possession are in fact different.

3.2. Reovirus can replicate in primary *ex vivo* malignant glioma surgical specimens

To determine if reovirus oncolysis occurred in brain tumor specimens taken from patients and was not confined to established cell lines, we tested 9 *ex vivo* brain tumor surgical specimens (Figure 3.4). The 9 glioma cell lines were derived from 4 GBMs, 3 anaplastic astrocytomas, 1 non-anaplastic astrocytoma and 1 oligodendroglioma. A spectrum of tumors was tested ranging from aggressive glioblastomas to benign meningiomas. Reovirus was able to infect and kill all 9 (100%) primary glioma cultures (top panel). No cell killing or morphological effects were observed in live and dead virus-infected cultured meningiomas. Furthermore, viral proteins were detected in live virus treated glioma cells using indirect immunofluorescent microscopy. GFAP staining of cultured cell lines confirmed their glial lineage. It is worth mentioning that although it has been assumed that the cells cultured are in fact gliomas, it remains possible that the cells may in fact be normal astrocytes as they too would be stained by GFAP.

To demonstrate further that viral protein synthesis was occurring in primary specimens [^{35}S] -methionine labeling was performed. Reovirus proteins were expressed in live virus-treated primary samples but not in the dead virus-infected controls (Figure 3.5). When compared to the levels of reovirus expressed in established cell cultures the levels of viral proteins present in primary cultures were comparable. These results show that reovirus is able to replicate in, and kill gliomas in primary cultures and oncolysis/replication is not unique to established cell glioma lines.

Figure 3.4. Effects of reovirus on brain tumor samples grown *ex vivo*. Immunofluorescence assay of viral proteins (*top panel*) expressed in reovirus-infected human primary glioma cell lines. Cells were infected with an estimated MOI of 10 PFU/cell. At 48h post-infection, cells were fixed, processed and reacted with rabbit anti-reovirus type 3 antibody and then with FITC-conjugated goat anti-rabbit immunoglobulin G. Results show viral proteins within primary glioma cell cultures. The magnification for all panels is 200X. GFAP staining (*bottom panel*) of primary glioma samples confirmed their glial lineage [GBM = glioblastoma].

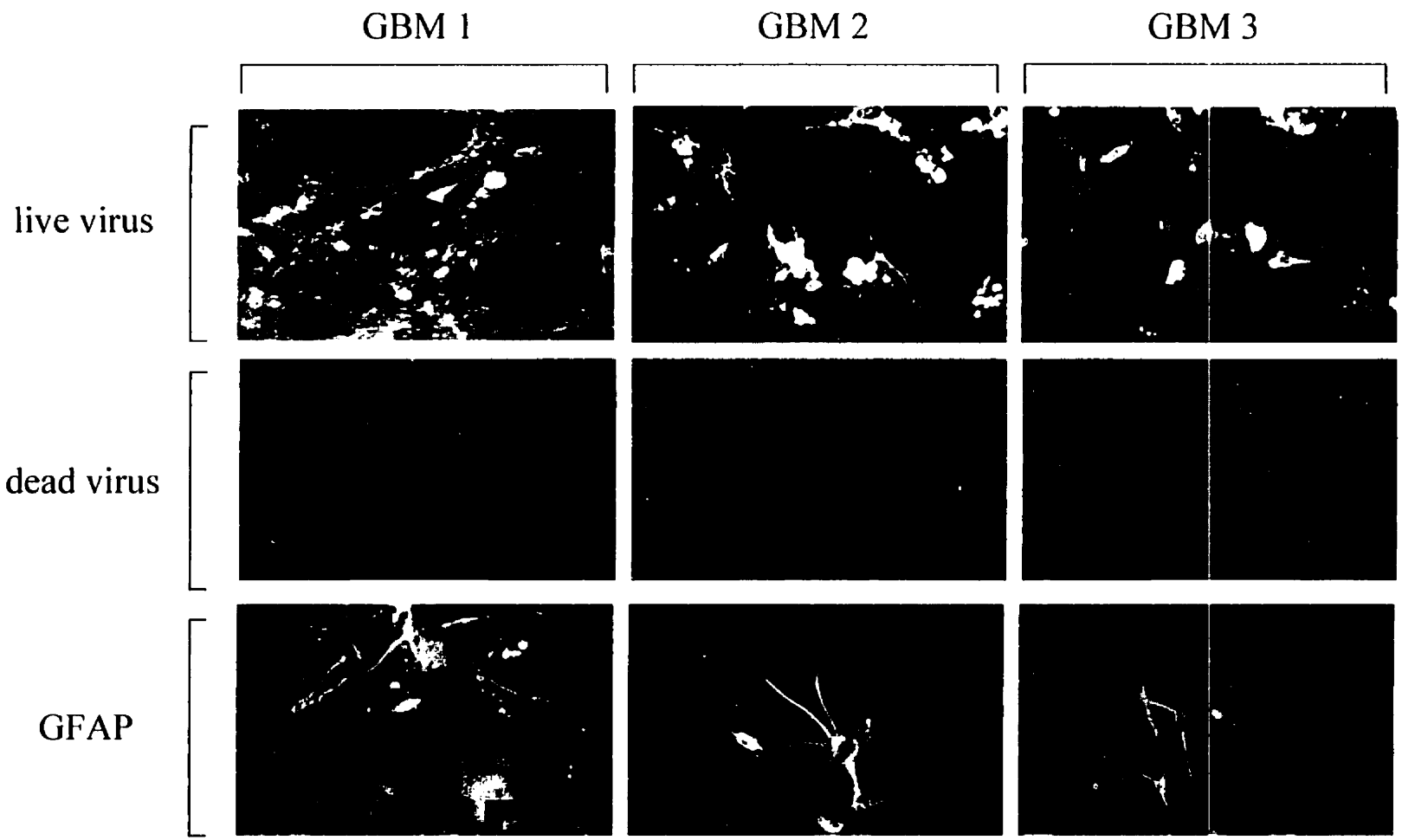
GBM 1
GBM 2
GBM 3
live virus
dead virus
GFAP

Figure 3.5. Reovirus protein synthesis in mock-infected and reovirus-infected primary brain cancer cell lines. Cells were labeled with [^{35}S] -methionine from 12 to 48 hrs post-infection (MOI = 10 PFU/cell). Lysates were then prepared and analyzed directly by SDS-PAGE. The positions of reovirus proteins (3 size groups: λ, μ, and σ) are indicated on the right. These results show that reovirus infection is not unique to established cell lines but also infects and kills glioma specimens removed from patients [GBM = glioblastoma; + = infected; - = mock-infected].

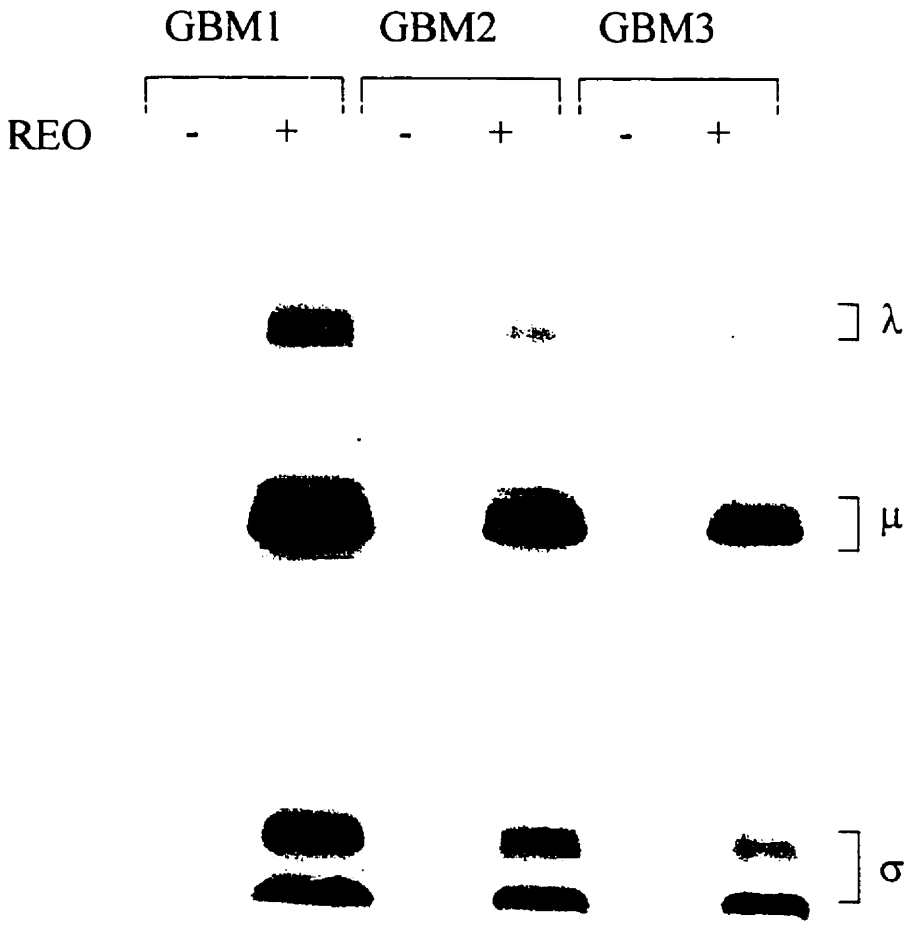
GBM1
GBM2
GBM3
REO
-
+
-
+
-
+
λ
μ
σ

3.3 Viral cytotoxicity of normal human fetal astrocytes and neurons

Reovirus was found capable of infecting cell cultures of normal fetal astrocytes and neurons provided by Dr. Voon Wee Yong. Specific antibodies to astrocytes (GFAP) and neurons (MAP-2) confirmed their lineage. Both astrocytes (Figure 3.6) and neurons (data not shown) were susceptible to reovirus infection. Following 48, 72 and 120 hrs post-infection with either live or dead virus, the morphology of the infected and mock-infected cell lines was compared by indirect microscopy. Both human fetal astrocytes and neurons were infected and killed by reovirus, however at a much slower rate than the established cell lines tested. By 48 hrs post-infection the majority of glioma cell lines were killed by reovirus, whereas 120 hrs of exposure to reovirus was required for fetal astrocytes to exhibit as dramatic of a cytopathic effect. The detection of viral proteins was carried out by indirect immunofluorescent microscopy (data not shown). Pronounced immunofluorescence was seen in both the reovirus-treated fetal astrocytes and neurons by 72 hrs post-infection.

To demonstrate further that these cell lines were capable of viral protein synthesis cells were labeled continuously for 12-48 hrs post-infection at which time they were analyzed by SDS-PAGE (Figure 3.7A). Again, results clearly show that these lines synthesized viral proteins and then were subsequently killed by reovirus. MAPK was also found activated in both fetal astrocyte and neuronal cell lines (Figure 3.7B and C).

Figure 3.6. Cytopathic effect of reovirus on primary fetal astrocytes. Confluent monolayers of cells were infected with reovirus at a MOI of approximately 50 PFU/cell. Pictures shown were taken at 48, 72, and 120 hrs post-infection for both reovirus-infected and mock-infected cells.

Figure 3.6.

Figure 3.7. (A) Reovirus protein synthesis in mock-infected and reovirus-infected normal human fetal astrocytes. Cells were labeled with [^{35}S] -methionine from 12-48 hrs post-infection (MOI = 50 PFU/cell). Lysates were then prepared and analyzed directly by SDS-PAGE. The positions of reovirus proteins are indicated on the right. [+ = infected: - = mock-infected] **(B)** MAPK phosphorylation as an indicator of susceptibility to reovirus infection. Fetal astrocytes and fetal neurons were plated in a six well plate. Cells were either grown in the presence of 10% FBS or were serum starved (0.5% FBS) for a 48 hour. Monolayers were washed in PBS and cell lysates were prepared and subjected to SDS-PAGE. Following blotting onto nitrocellulose paper, samples were probed samples were probed with antibodies directed against phospho-MAPK. Phospho-MAPK levels were all standardized by total MAPK levels. Both astrocytic and neuronal cell lines showed high levels of MAPK activation, as they were also found susceptible to reovirus infection. [FA = fetal astrocytes; FN = fetal neurons] (C) Total MAPK levels in fetal astrocytic and neuronal cell lines.

A.

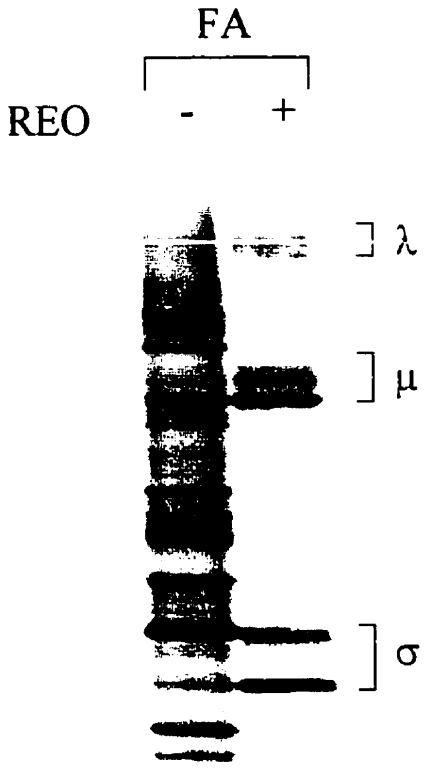

B. Phospho-MAPK

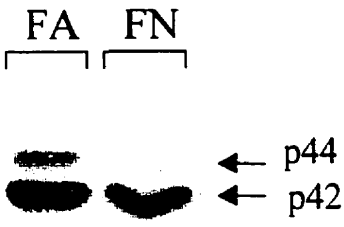

C. Total MAPK

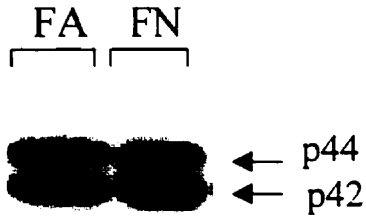

3.4. Reovirus causes tumor regression of human malignant gliomas in a subcutaneous SCID NOD mouse model

SCID NOD mice bearing subcutaneous human malignant gliomas mice were treated with a single injection of live or dead (UV-inactivated) reovirus and tumor area was measured twice weekly beginning on "Day 0" (Figures 3.8A and B). In Figure 3.8A, the results of live and dead virus-treated U251N xenografts clearly demonstrate a striking inhibition and regression of reovirus treated tumors. A significant difference in tumor size between the two groups was apparent by Day 7 (0.24 cm^2 ± 0.0991 versus 0.53 ± 0.0318 cm^2; t-test, p=0.0013) and remained until Day 21 when both groups needed to be sacrificed. The control group was sacrificed because the mice became moribund from tumor growth. Impressive anti-tumor activity using reovirus against the human malignant glioma cell line U87 was also seen in the same model (Figure 3.8B). On Day 14, a difference in tumor size was seen between the live and dead virus groups (0.36 cm^2 ± 0.0085 versus 0.55 cm^2 ± 0.0299; t-test, p=0.0014).

Histological examination of any remaining subcutaneous "mass" found no microscopic evidence of residual tumor (Figure 3.9). In contrast, all dead virus treated animals had large, actively proliferating tumors. No evidence of viable tumor cells or tumor infiltration into the underlying skeletal muscle was seen in the live virus-treated tumor group (as compared to the control). Immunofluorescent analysis of paraffin sections of the live virus-treated tumor using anti-reovirus antibodies showed that reovirus replication was restricted to the tumor mass and myocardium without spreading to the underlying normal tissue and therefore cell killing occurred through reovirus infection (data not shown). Reovirus proteins were not detectable in the tumor treated with UV-inactivated virus nor were they found in other tissues (brain, kidney, lung, liver, spleen; Figure 3.10).

As expected, we encountered some significant toxicities in SCID NOD mice. In the 80% of the live virus group (both cell lines) the hind limbs of the mice became black and necrotic bilaterally after approximately 21 Days (at which time the tumors had regressed

and been "cured"; this was not seen in dead virus-treated mice). Initially, we wondered if this was specific for glioma lines in general however, this toxicity was also seen with the breast cancer cell line MDAMB468. Preliminary histologic analysis of the affected limbs showed what could be a necrotizing vasculitis but to this date this toxicity has not been properly characterized nor its mechanism determined. It is important to note that these limb toxicities were not observed when experiments were repeated using nude mice. In addition, all live virus-treated animals developed focal myocarditis (Figure 3.10). Inflammation was not however prominent, at least by the time the myocardium was examined. Reovirus-induced myocarditis consisted acutely of scattered polymorphonuclear cells and then subsequently of lymphocytes and macrophages in later stages of infection.

Figure 3.8. Effect of reovirus on U251N or U87 human tumor xenografts grown subcutaneously in SCID NOD mice. **(A)** The human glioblastoma cell line, U251N was introduced as a tumor xenograft subcutaneously into a site overlying the hind flank of SCID NOD mice. Following palpable tumor establishment (after approximately 2 weeks) a single intratumoral injection of 1.0×10^7 PFUs of reovirus serotype 3 was administered. Control animals were given an intratumoral injection of dead (UV-inactivated) reovirus. A striking inhibition, and regression of reovirus treated tumors was seen. A significant difference in tumor size between the two groups was apparent by Day 7 (0.24 ± 0.014 cm^2 versus 0.53 ± 0.094 cm^2 respectively; t-test, $p = 0.0013$ (day 21); $n = 10$) and persisted until sacrifice. **(B)** Similar results were obtained using the U87 malignant glioma cell line. On Day 14, a difference in tumor size can be seen between the live and dead virus-treated groups (0.36 ± 0.0235 cm^2 versus 0.55 ± 0.028 cm^2 respectively; t-test, $p = 0.0014$ (day 29); $n = 10$). In experiments A and B, 80% of the live virus animals developed black and necrotic hind limbs after 21 days at which time the tumors had regressed and possibly been "cured". This toxicity was not seen in any of the dead virus-treated animals.

A.

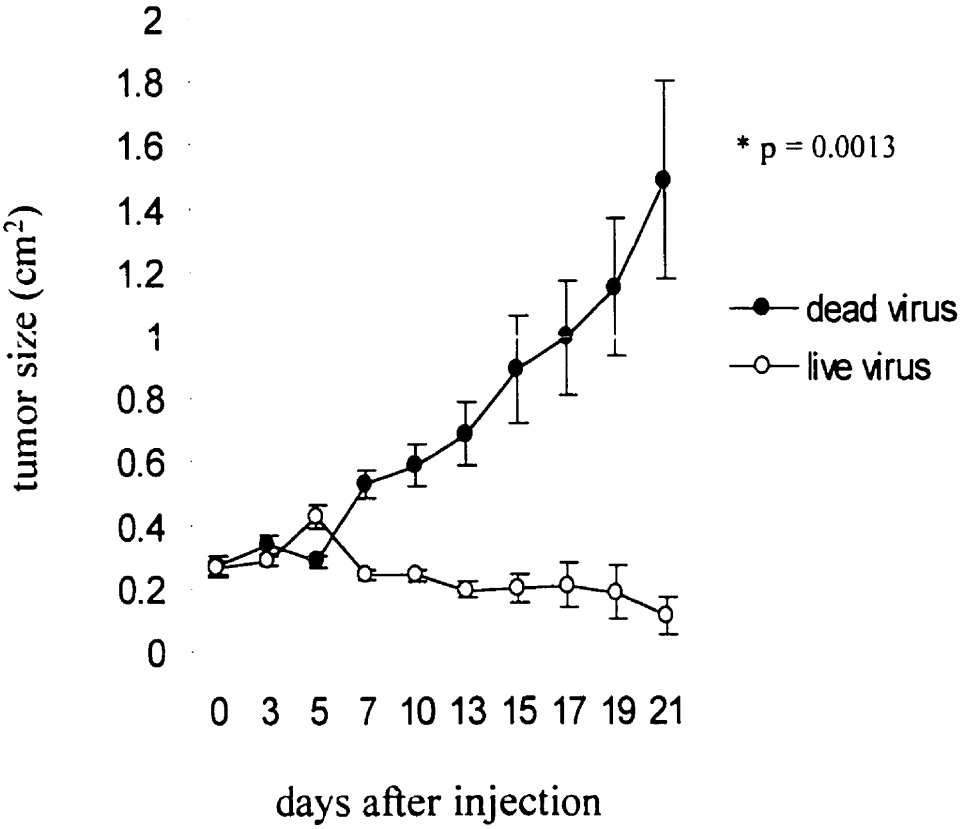
2
1.8
1.6
1.4
1.2
1
0.8
0.6
0.4
0.2
0
tumor size (cm²)
* p = 0.0013
dead virus
live virus
0 3 5 7 10 13 15 17 19 21
days after injection

B.

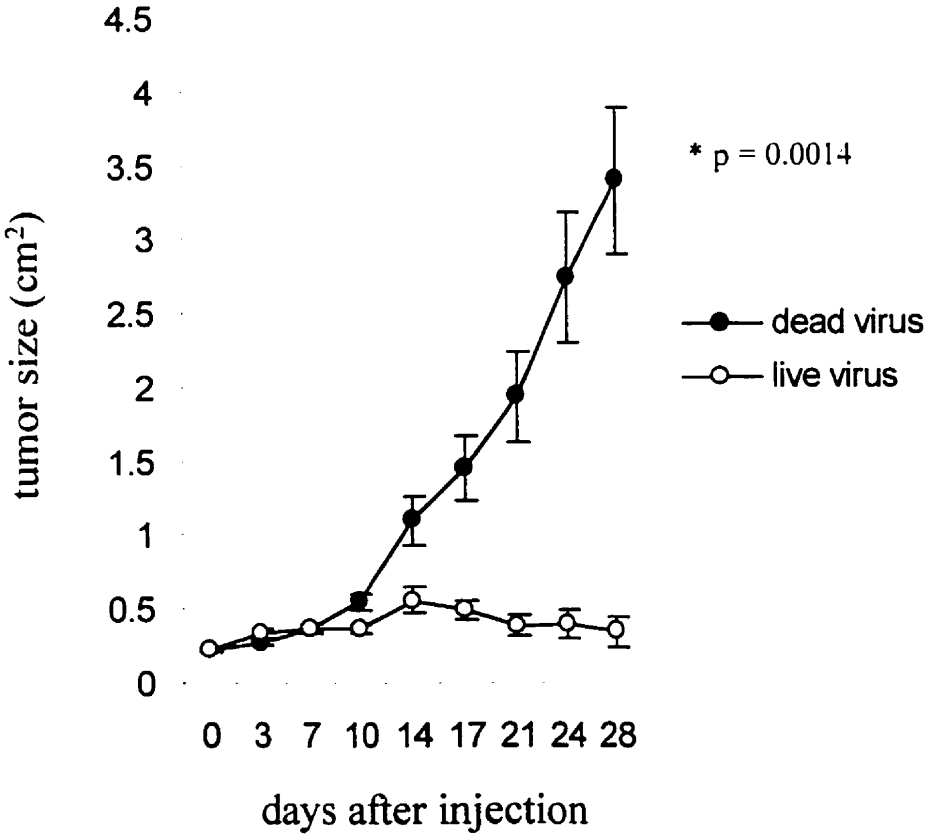
4.5
4
3.5
3
2.5
2
1.5
1
0.5
0
tumor size (cm²)
* p = 0.0014
dead virus
live virus
0 3 7 10 14 17 21 24 28
days after injection

Figure 3.9. H&E staining of the remaining subcutaneous tumor mass 4 weeks after treatment with live or dead (UV-inactivated) virus (*top panel*). There was no evidence of viable tumor cells or tumor infiltration into underlying skeletal muscle in the reovirus-treated tumors. However significant toxicities were observed in animals that received reovirus treatment. At autopsy there was evidence of hind limb necrosis, possibly consistent with immune mediated vasculopathy, as well as myocarditis (*bottom panel*).

dead virus (40X)

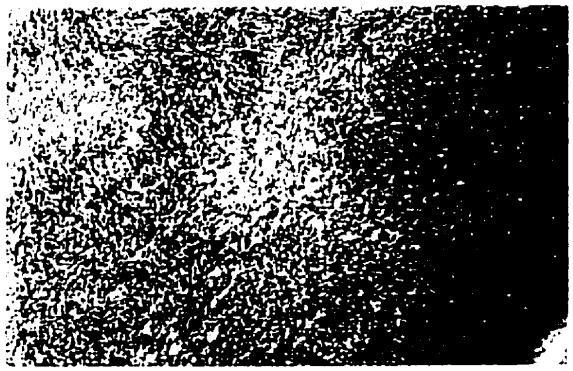

live virus (40X)

live virus (100X)

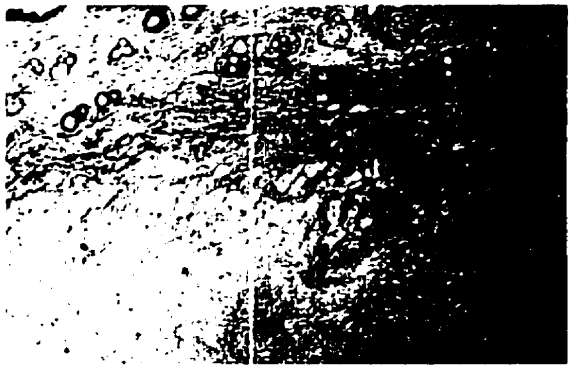

heart (40X)

heart (100X)

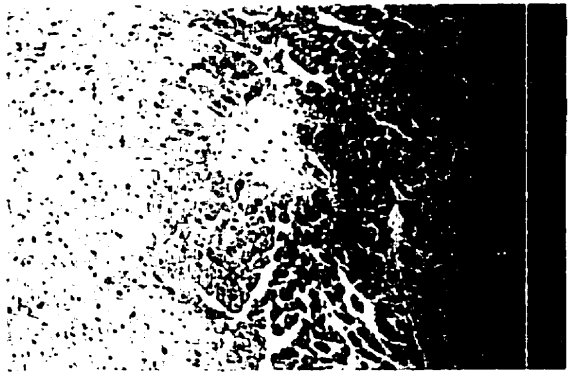

Figure 3.10. Immunofluorescence analysis of paraffin sections against total reovirus proteins showed viral proteins to be present in the reovirus treated tumor and the myocardium but not in other tissues (spleen, lung, liver, and kidney). Tissues were fixed, processed and reacted with rabbit anti-reovirus type 3 antibody and then with FITC-conjugated goat anti-rabbit immunoglobulin G (sections were counterstained with Evan's blue). Virus replication was restricted primarily to the tumor mass and did not spread to the underlying normal tissue. Reovirus proteins were not detected in any organs of the dead virus-treated animals (data not shown).

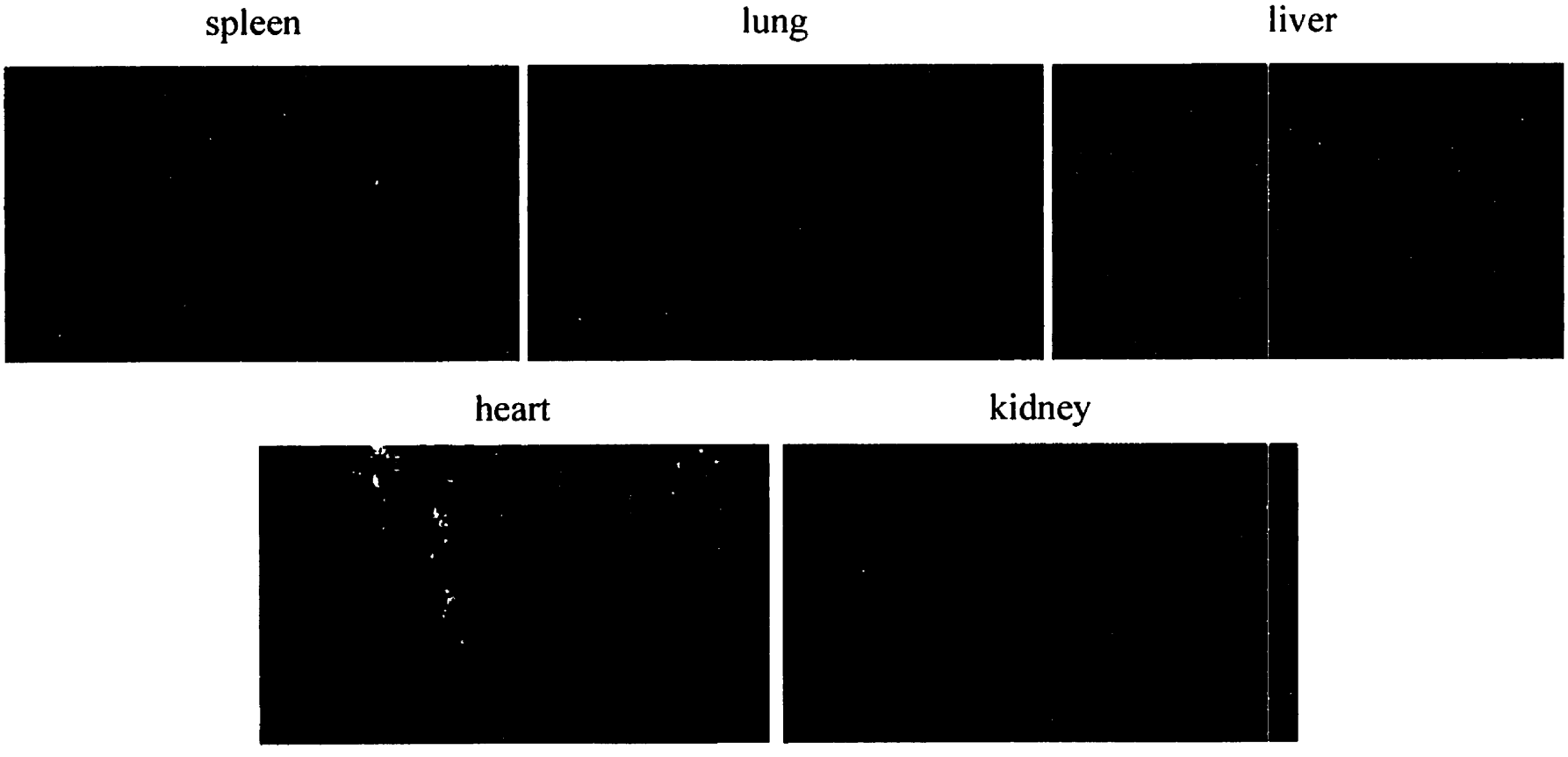
spleen
lung
liver
heart
kidney

3.5. Effect of reovirus on an intracerebral model of human malignant gliomas in immunodeficient mice

In human malignant glioma cells (U251N or U87lacZ) implanted intracerebrally and treated with a single intratumoral inoculation of reovirus, a significant difference in tumor size was evident between live and dead virus treated groups. Representative cross sections of both groups are shown in Figure 3.11A. The top panel sections are stained with H&E and the bottom is stained for β-gal in order to facilitate the identification of invasive or isolated tumor cells. The percentage of the brain hemisphere occupied by tumor was dramatically reduced in the live virus group compared to that of the dead virus controls (U251N: 3.2% ± 0.53 versus 38.3% ± 6.22; t-test, $p = 0.0026$. U87lacZ: 2.4% ± 0.63 versus 40.5% ± 7.97; t-test, $p = 0.0048$) (U87lacZ: Figure 3.11B). This experiment was done to show reovirus was effective intracerebrally as a "proof of concept". As expected, all live-virus treated animals became sick (subjectively and from body weight) and needed to be sacrificed whereas all dead virus-treated animals remained well. The animals were sacrificed in pairs (i.e. a dead virus animal was sacrificed at the same time as a live virus animal) so that differences in tumor size between animal "pairs" would not be confounded by differences in survival time. H&E staining of the remaining tumor "mass" four weeks following live reovirus treatment delivered intratumorally into either U251N or U87lacZ intracranial tumors showed few viable tumor cells still to be present in the brain (U87lacZ: Figure 3.12). If animals had survived a greater length of time then tumors may have had time to completely regress as a result of live virus treatment.

Figure 3.11. Effects of intratumoral reovirus treatment administered intracerebrally to the human malignant glioma cell lines U251N or U87lacZ. 5×10^4 U87lacZ cells were implanted stereotactically in the right putamen of SCID NOD mice. Two weeks later a single injection of 10^7 PFUs of live or dead (UV-inactivated) reovirus was delivered stereotactically i.t. (A) Representative coronal H&E sections of SCID NOD mouse brains with U87lacZ tumors (*top*) and X-gal stained (*bottom*) show a marked reduction in tumor size in the live virus-treated group. (B) The size of the intracerebral tumors was dramatically reduced in the live virus-treated group as compared to the control group (U251N: 3.2% ± 0.53 versus 38.3% ± 6.22 of the brain hemisphere; t-test. $p = 0.0026$. U87lacZ: 2.4% ± 0.63 versus 40.5% ± 7.97 of the brain hemisphere; t-test, $p = 0.0048$; $n = 10$ for each group).

A.

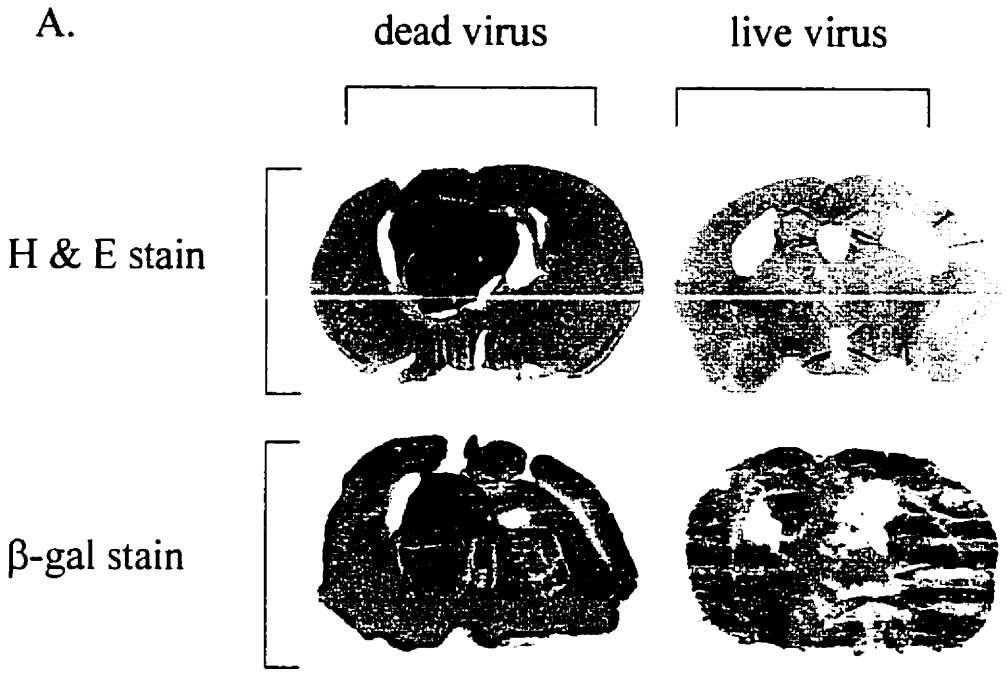
dead virus
live virus
H & E stain
β-gal stain

B.

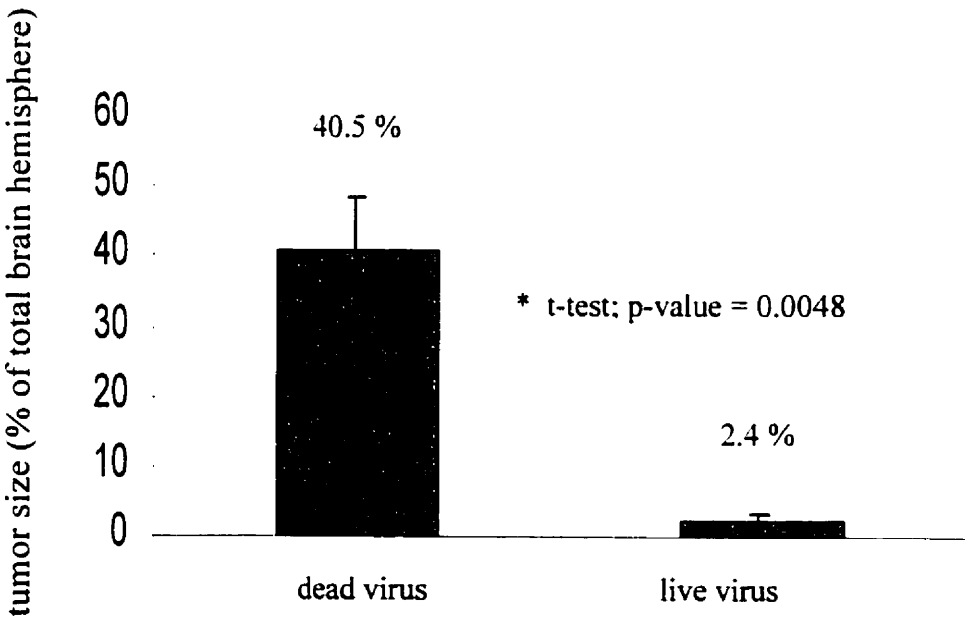
tumor size (% of total brain hemisphere)
60
50
40
30
20
10
0
40.5 %
* t-test: p-value = 0.0048
2.4 %
dead virus
live virus

Figure 3.12. Effects of reovirus treatment delivered intratumorally to U87 human malignant glioma implanted intracerebrally in SCID NOD mice. H&E staining of the remaining U87 i.c. tumor mass 4 weeks after treatment of live (d,e,f) and dead (a,b,c) virus [a,d:25X; b,e:40X; c,f: 100X]. Few viable tumor cells remained following histological examination of the brains of the reovirus treated animals.

C.

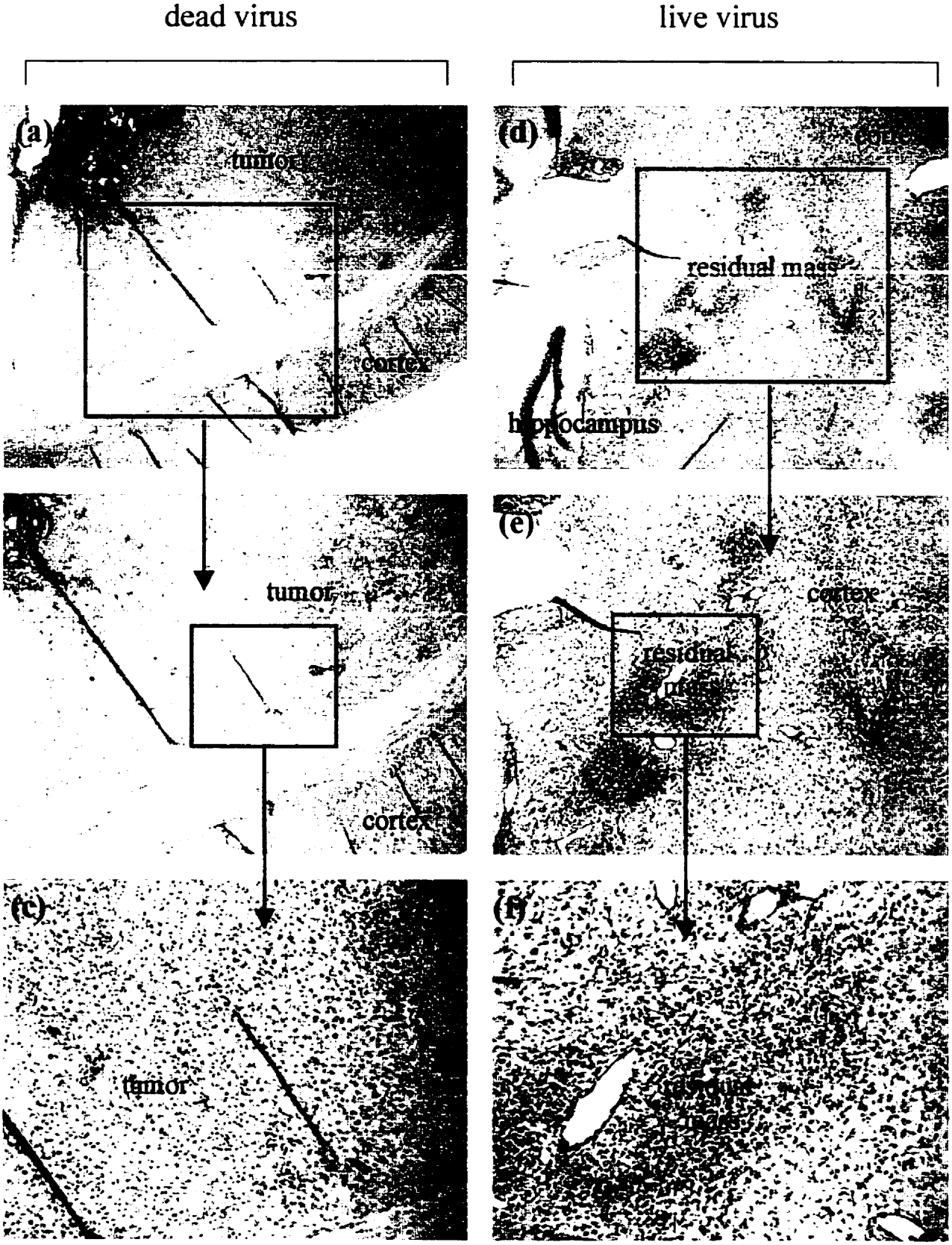
dead virus
live virus
(a)
tumor
cortex
(b)
tumor
cortex
(c)
tumor
(d)
residual mass
hippocampus
(e)
cortex
(f)

3.6. Reovirus causes tumor regression in a subcutaneous immunocompetent animal glioma model

A potential challenge to viral therapeutics is the host immune system, which could inactivate viruses with host antibodies. We examined the effects of reovirus on the growth of 9L allografts in Fischer 344 rats (Figure 3.13A). In rats treated with live or dead virus, tumor area was measured thrice weekly beginning on "Day 0" (Figure 3.13B). Due to the presence of a competent immune system, the rats were given a series of intratumoral injections of reovirus over 21 days (6 injections of 10^8 PFUs each for the first 7 days, followed by injections of 10^7 PFUs every 2 days for the next 14 days). The control group was injected with equivalent amounts of dead virus. After 14 Days of treatment there was a significant difference in tumor size (3.7 ± 0.235 cm^2 versus 8 ± 0.933 cm^2; t-test, $p = 0.0001$ (day 21)). Repeated administration of virus caused the subcutaneous tumors to become quite soft and spongy. Dissection on the day of sacrifice showed most "tumors" to be fluid filled sacs without any underlying solid tumors. The cutaneously measured "tumor" areas therefore grossly overestimated the true tumor size. On Day 21, complete regression of palpable tumors was seen in 7 of 16 (43%) reovirus treated rats and no residual tumor was found histologically. In the other 9 of 16 (56%) animals that had palpable "tumors" of various sizes no histological evidence of tumor was found in 4 (25 %). The other 5 tumors (31 %) had varying sizes of tumor nodules, all of which were smaller than the tumors from the dead virus group. Therefore, 11/16 (69 %) animals had complete tumor regression clinically and on histologic examination. This experiment was repeated once and similar results were obtained.

Figure 3.13. Effect of reovirus on rodent 9L cells grown subcutaneously in Fischer 344 immune-competent rats. **(A)** Photographs of live and dead virus-treated animals, at the time of sacrifice. **(B)** Immunocompetent Fischer 344 rats were implanted with a single syngeneic 9L graft. Following tumor establishment, animals were given a series of intratumoral injections of reovirus (open circles: n = 16 tumors) or dead reovirus (closed circles: n = 12 tumors). After 14 days of treatment, a significant difference in tumor size between the two groups can be seen. By Day 21, complete tumor regression was seen in 7 of 16 (43%) of reovirus treated rats. Histologic examination of tumor-host architecture of the remaining tumor foci showed 11/16 (69%) to have been cured.

A.

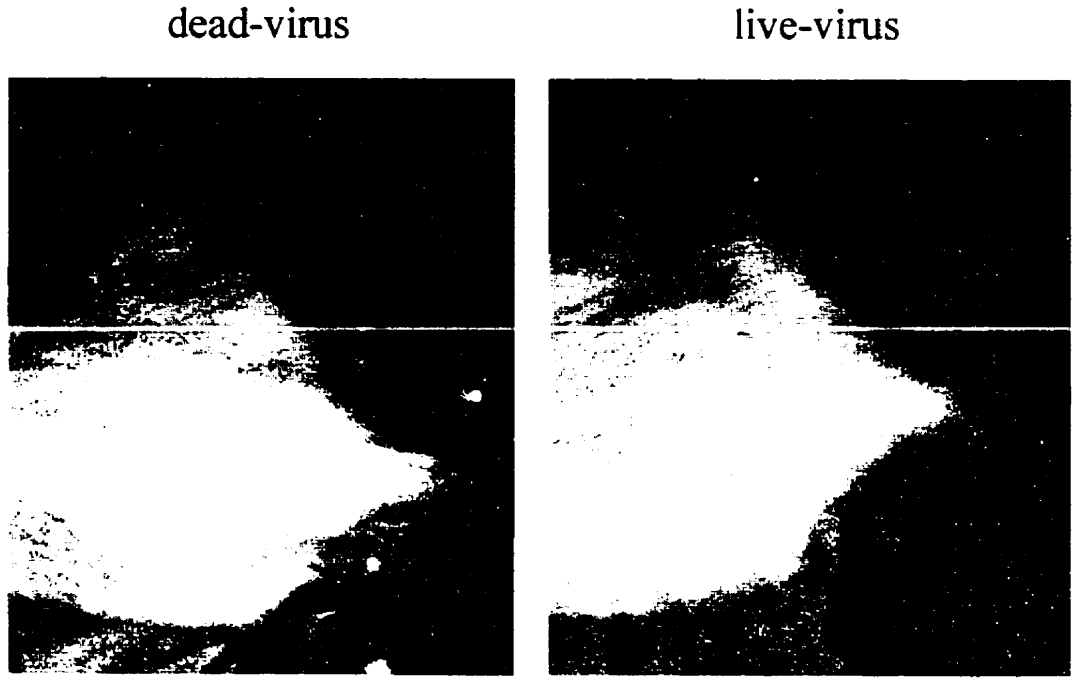
dead-virus
live-virus

B.

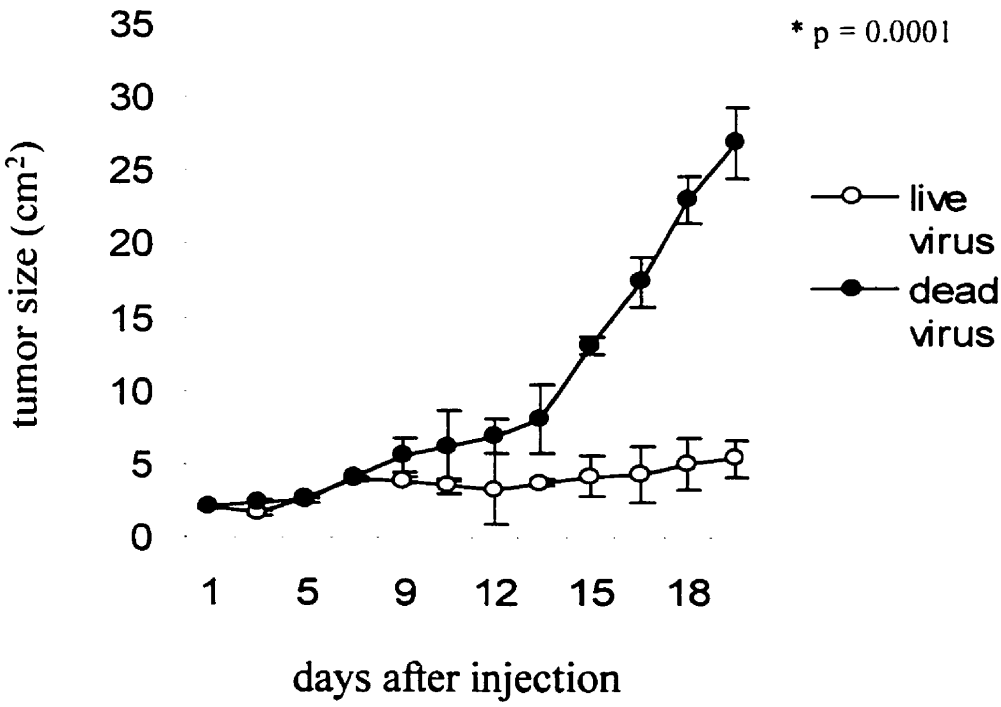
* p = 0.0001
tumor size (cm²)
35
30
25
20
15
10
5
0
1
5
9
12
15
18
days after injection
live virus
dead virus

3.7. In the presence of pre-existing, circulating antibodies reovirus causes tumor regression in an immunocompetent animal glioma model

We next determined if pre-existing antibodies to reovirus would abrogate the oncolytic effects of the virus. Anti-reovirus antibodies were raised in Fischer rats following challenge with an intramuscular injection of reovirus (10^7 PFUs). These animals were then implanted with 9L allografts subcutaneously and treated with reovirus for 27 days. Reovirus treatment consisted of 6 injections of 10^8 PFUs each for 7 days, followed by injections of 10^7 PFUs every 48 hours for the next 7 days; this 2-week treatment regimen was then repeated for the remaining 13 days. Previous exposure to reovirus did not affect the ability of the virus to destroy glioma tumor cells (Figure 3.14A). For example, on Day 27 the tumor sizes were dramatically different between the two groups (3.7 ± 2.5 cm^2 versus 19 ± 2.75 cm^2; t-test, $p = 0.001$). These results are similar to rats without anti-reovirus antibodies (i.e. Figure 3.13B) as 6 of 14 (43%) of the live virus treated animals were completely "cured" as no residual tumor was found histologically. The live-virus treated group remained healthy at the time of sacrifice as determined by consistent weight gain and normal physical appearance.

3.8. Reovirus causes glioma regression at sites distant from the site of virus administration in immunocompetent animals

A major barrier to effective glioma treatment is their highly invasive nature where invasive glioma cells are found several centimeters away from the main tumor mass. We determined if reovirus would kill glioma cells remote from the site of viral administration (Figure 3.14B) in immunocompetent animals. Immunocompetent Fischer 344 rats were implanted subcutaneously with bilateral 9L tumors. Following the establishment of both tumors, reovirus was administered i.t. to the ipsilateral tumor only (live virus ipsilateral) but not to the contralateral tumor (live virus contralateral) [injections of 10^9 PFUs of virus was given everyday for 29 days]. Dead virus was administered to the control group

and again only the ipsilateral (dead virus ipsilateral) tumor was injected. Tumor growth inhibition and regression were seen in live virus ipsilateral tumors. No contralateral tumors regressed completely but the difference in live and dead virus groups was significant (12 ± 4.42 cm^2 versus 21 ± 3.22 and 23 ± 2.34 cm^2; t-test, $p = 0.0087$ (day 29)). Immunohistochemical analysis confirmed that viral proteins were present in both ipsilateral and contralateral tumors confirming that cell killing occurred directly by reovirus infection. Reovirus was not detected in other tissues (brain, heart, liver, lung, kidney, or spleen).

Figure 3.14. *In vivo* effect of reovirus on local and remote glioma allografts. **(A)** Oncolytic effect of reovirus in rats with previous circulating reovirus antibodies. Fischer 344 rats were given a single intramuscular injection of reovirus and antibodies to reovirus were detected 2 weeks following. Rats were then implanted with 9L subcutaneously and tumors allowed to grow. Tumors in rats with previous exposure to reovirus injected were injected either with live (open circles: n = 15 tumors) or dead virus (closed circles: n = 15 tumors). Reovirus antibodies or previous viral exposure to reovirus did not affect glioma cell killing as 4/14 (35%) test animals were cured of their tumor. **(B)** *In vivo* effect of reovirus on remote glioma allografts. Immune-competent 344 rats were implanted with two 9L allografts overlying each of their hind flanks. Following the establishment of both tumors, reovirus treatment was administered intratumorally to the ipsilateral tumor **only** (open circles and triangles: n = 9). UV-inactivated virus was administered to the control group, again to the ipsilateral tumor **only** (closed circles and triangles: n = 8). Tumor regression, while not identical, was seen in the ipsilateral, injected tumor (live virus ipsilateral) and contralateral, uninjected tumor (live virus contralateral) following reovirus administration. This experiment was repeated once with similar results.

A.

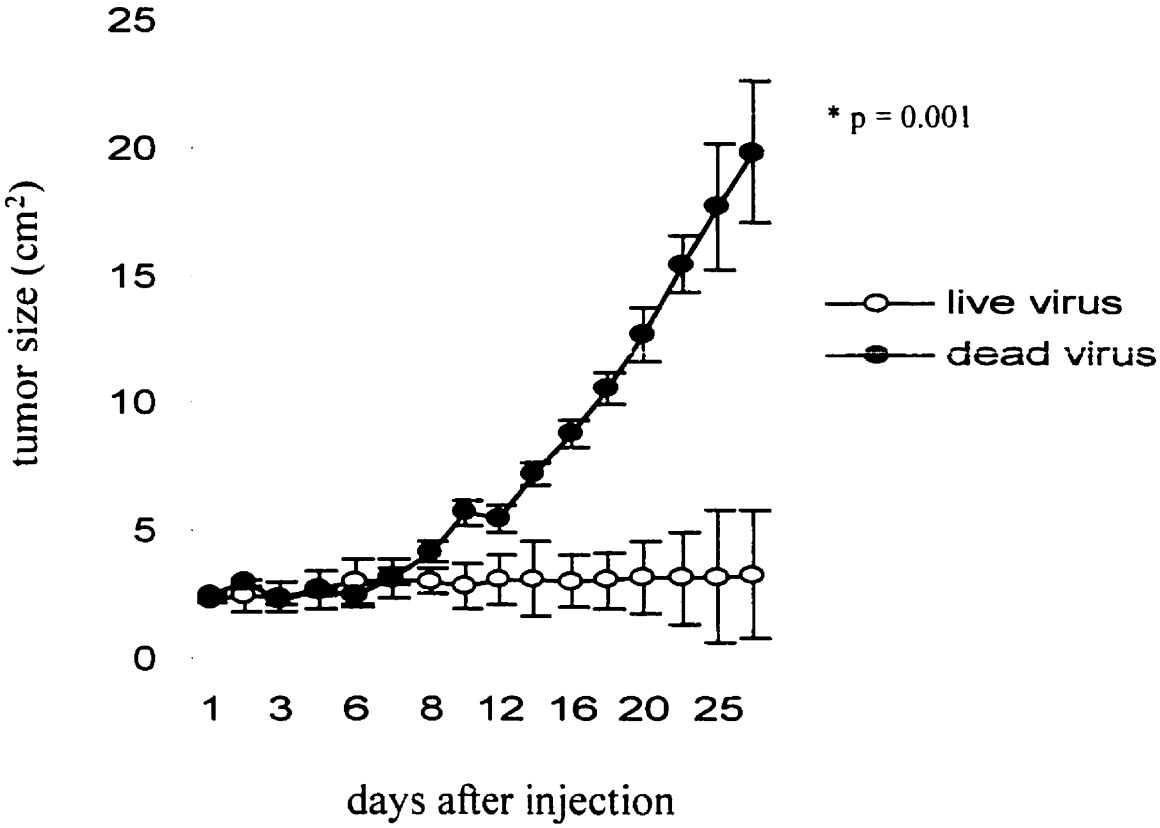
25
20
15
10
5
0
tumor size (cm²)
1 3 6 8 12 16 20 25
days after injection
* p = 0.001
live virus
dead virus

B.

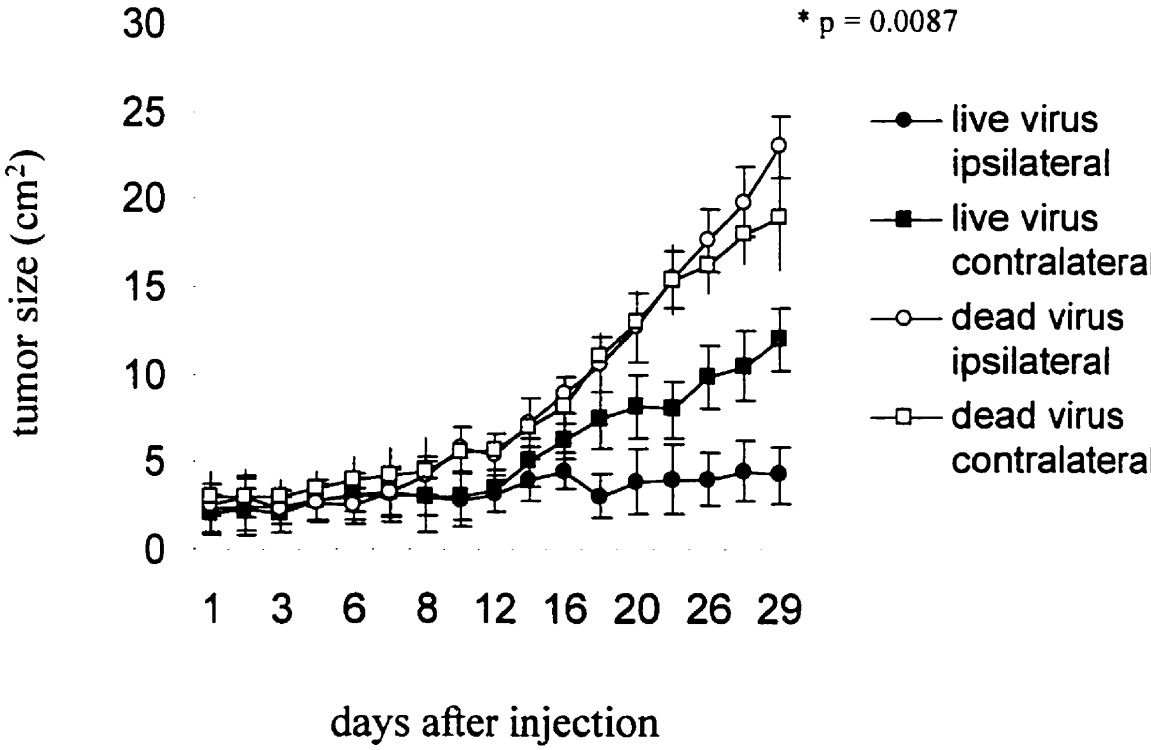
30
25
20
15
10
5
0
tumor size (cm²)
1 3 6 8 12 16 20 26 29
days after injection
* p = 0.0087
live virus ipsilateral
live virus contralateral
dead virus ipsilateral
dead virus contralateral

3.9. *In vivo* effects of reovirus injected intracranially in immunocompetent rats without tumors.

Virus (10^9 PFUs) was injected into the right putamen of Fischer 344 rats at time "0". At subsequent time points, beginning at 1 hr after infection, brains were harvested and the amount of reovirus as well as its location (local versus remote) in the both brain hemispheres was determined (Figure 3.15A). At 12 hrs post-infection, virus was found to be present by plaque titration in the ipsilateral (the hemisphere that received the injection) at 2.8×10^8 PFUs. In the contralateral (uninjected) hemisphere, at 12 hrs post-infection, the lytic capacity of recovered virus was found to be 3×10^7 PFUs when assayed on L929 cells. By 72 hrs post-infection, virus was found distributed at almost equivalent levels throughout the brain (7.8×10^7 PFUs in left versus 6.5×10^7 PFUs in right: 1×10^6 PFUs/mL of virus was found circulating in the blood stream on average). Histopathological examination of the live virus-treated brains showed mild inflammatory responses to viral infection in the brain. Further immunofluorescent analysis showed viral proteins present in activated microglia (confirmed by neuropathologist; NBR). A uniform pattern of virus distribution was evident by 72 hrs post-infection (Figure 3.15B). These results show that a generalized reovirus infection occurs in the brain fairly rapidly following intracranial inoculation.

Given that repeated injections of virus were required to reduce tumor burden in a subcutaneous location in immunocompetent Fischer 344 rats, we next needed to determine the 50% lethal dose (50% animals surviving; LD_{50}) of a 10^9 PFU dose inoculated into the brains of these animals. Animals (n = 5) receiving a **single** dose were entirely well (displayed normal behaviors and consistent weight gain) and were electively sacrificed at 3 months following infection. Subsequent histological examination of the **live** virus-treated brains showed no evidence of abnormal histology when compared with that of the control group (injected with PBS; Figure 3.15C). Immunofluorescence analysis showed no evidence of persistent viral replication. In a second experiment (n =

10), animals were repeatedly administrated 10^9 PFUs of reovirus every 48 hrs until it was determined that animals had to be sacrificed (i.e. they were unresponsive to touch or exhibited consistent weight loss; Figure 3.16A). Following the 3 dose administrations 5/10 (50%) of the live virus-treated animals had to be sacrificed. Given the difficulty of administering virus through a small cannula, animals were anaesthetized for each injection with halothane. One dead virus- and one live virus-treated animal did not survive the stress of the anaesthetic following a fifth dose. Gram staining showed co-existent bacteria-induced encephalitis to be present in the brains of these animals. Whether this infection was in fact caused the death of the live virus-treated animals in currently under investigation. Bacterial infection could possibly have been the result of the cannula system where repeated wound opening was required to administer virus through the cannula. The observation that bacteria were more commonly present in the live virus-treated animals (9/10) had a positive gram stain versus the dead virus-treated animals (4/10) suggests the possibility that reovirus administered intracerebrally could predispose the animals to a bacterial meningo-encephalitis.

Figure 3.15. (A) Titers of reovirus produced in Fischer rats inoculated with a single injection of reovirus intracerebrally at various times post-infection. 1 x 10^9 PFUs of reovirus was stereotactically injected into to right putamen of Fischer rat brains. The brains were then harvested at various indicated times, split in half and virus yields were determined by plaque titration on L929 cells. (Virus titer at time 0 was 1 x 10^6 PFU/mL) **(B)** Immunofluorescence of representative sections of virally infected brains at 72 hrs post-infection shows viral protein along the needle tract as expected (left). Stimulated microglial cells, activated in response to a presumed virally (or bacterially)-induced immune response, show viral proteins to be present (right). Magnification for pictures was 40X (*left*) and 100X (*right*). **(C)** Representative sections of both dead (*left*) and live (*right*) virus-treated brains following a single injection of 10^9 PFUs of reovirus administered intracerebrally. Animals (n = 5) were electively sacrificed 3 months after virus injection. Histologic examination of the brains of both live and dead virus-treated animals were normal and showed no evidence of chronic active inflammation or other pathology. Chronic inflammation would have been demonstrated by the presence of macrophages and CD8+ T cells at the original tumor site, in addition to microglia and astrocyte activation in the brain following reovirus therapy but was not seen using this route and schedule of administration. Magnification 100X.

A.

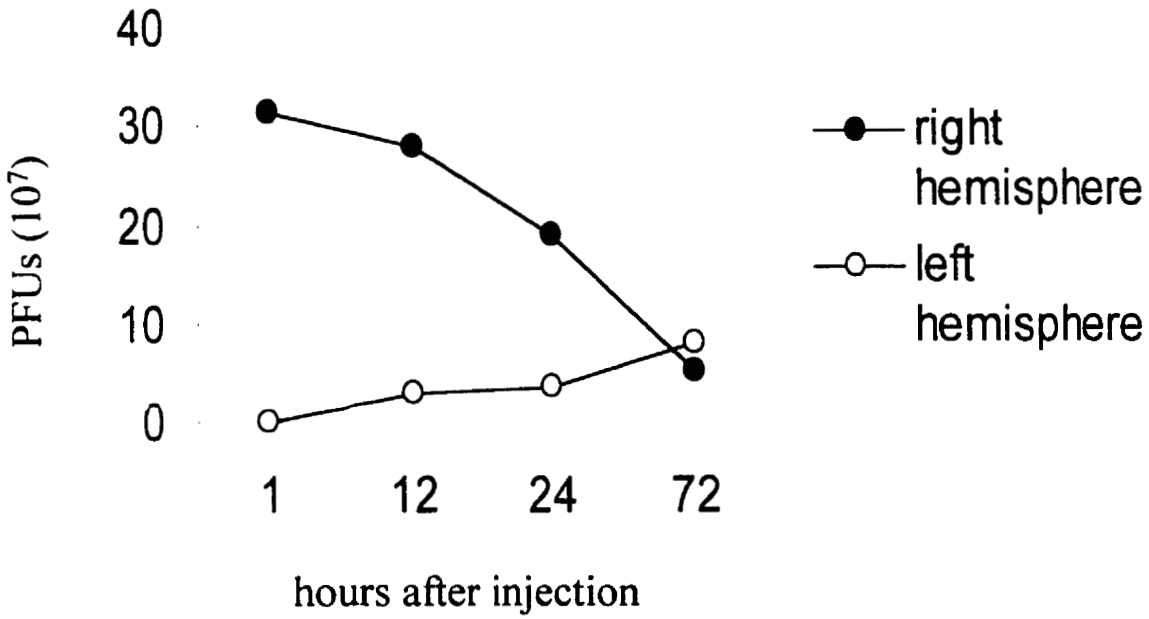
40
30
20
10
0
PFUs (10^7)
1
12
24
72
hours after injection
right hemisphere
left hemisphere

B.

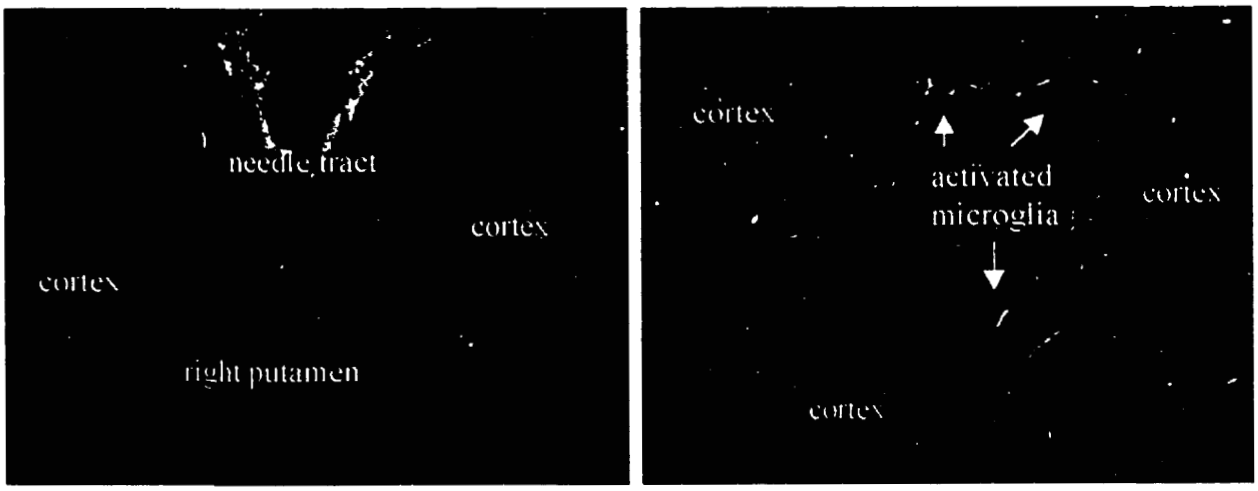
needle tract
cortex
cortex
right putamen
cortex
activated microglia
cortex
cortex

C.

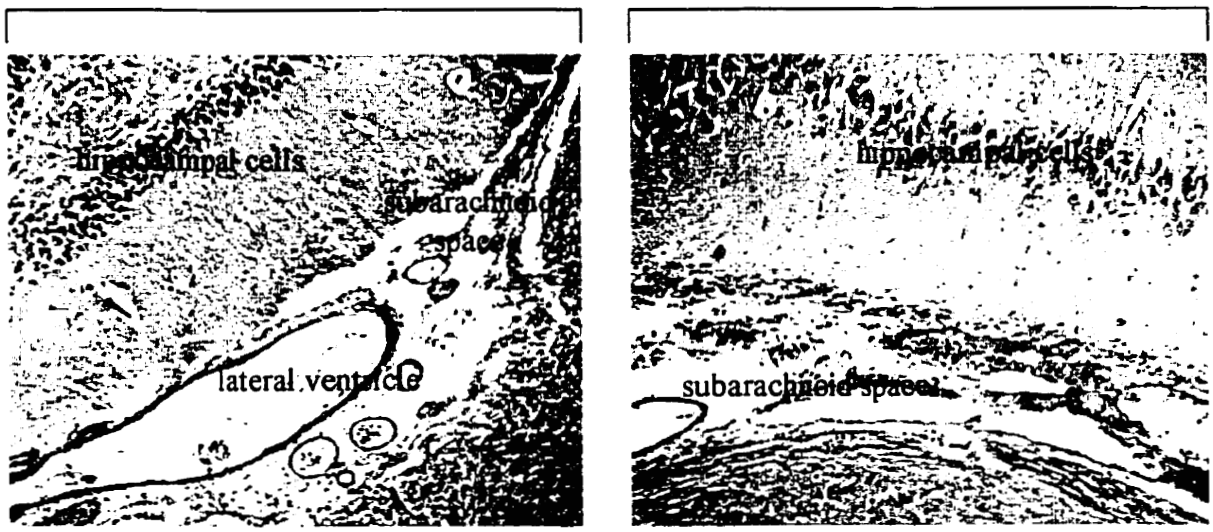
dead virus
live virus
hippocampal cells
subarachnoid space
lateral ventricle
hippocampal cells
subarachnoid space

Figure 3.16. **(A)** Survival plot for the percentage of Fischer rats with 9L intracranial tumors surviving repeated intracranial reovirus administration through an intracranial cannula. Animals were injected every 48 hours with 10^9 PFUs of reovirus until they died or had to be sacrificed because of behavior changes or consistent weight loss. Animals were given 3 doses of 10^9 PFUs of reovirus at which time 5/10 animals (50%). Therefore, LD_{50} of 10^9 PFUs given i.c. through a chronic indwelling cannula was 3 doses. **(B)** H&E sections (a,b) of live virus-treated brains following repeated intracerebral reovirus administration. Histologic examination showed a possible virally-induced encephalitis evident by focal neuronal loss and phagocytosis, lymphocytic "cuffing" of vessels with an increase in microglial cells in response to the local inflammatory response as well as an astrocytic reaction (increase in number and size of astrocytes in response to the loss of neurons). Gram staining of these brains (c,d) showed bacteria to be present throughout the subarachnoid space. Bacterial colonies (shown by blue staining) were not limited to the live virus-treated animals however their population was much more dense then that seen in the brains of dead virus-treated controls. Magnification 40X (*a,c*) and 100X (*b,d*).

A.

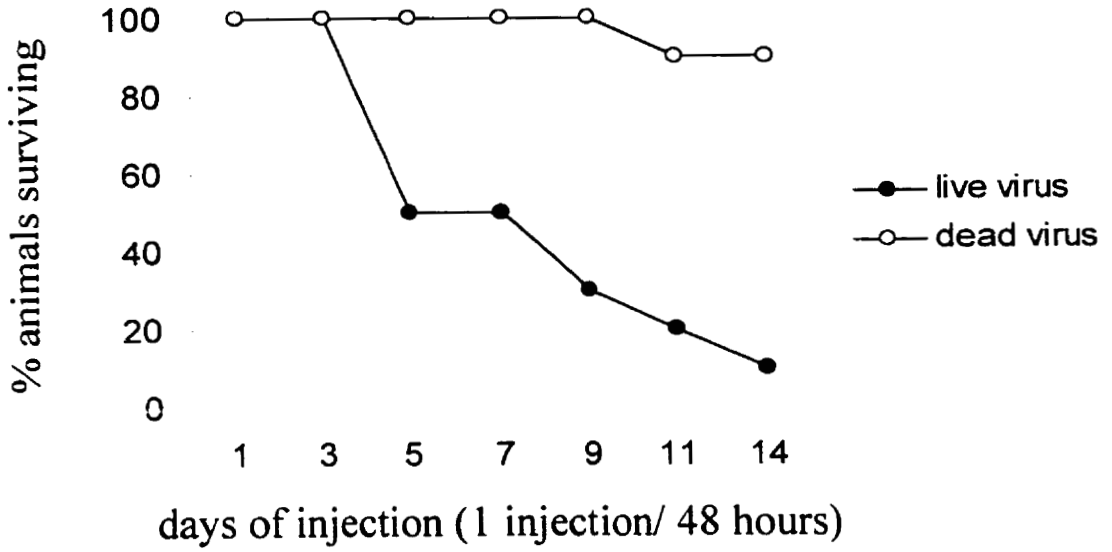
100
80
60
40
20
0
% animals surviving
1
3
5
7
9
11
14
live virus
dead virus
days of injection (1 injection/ 48 hours)

B.

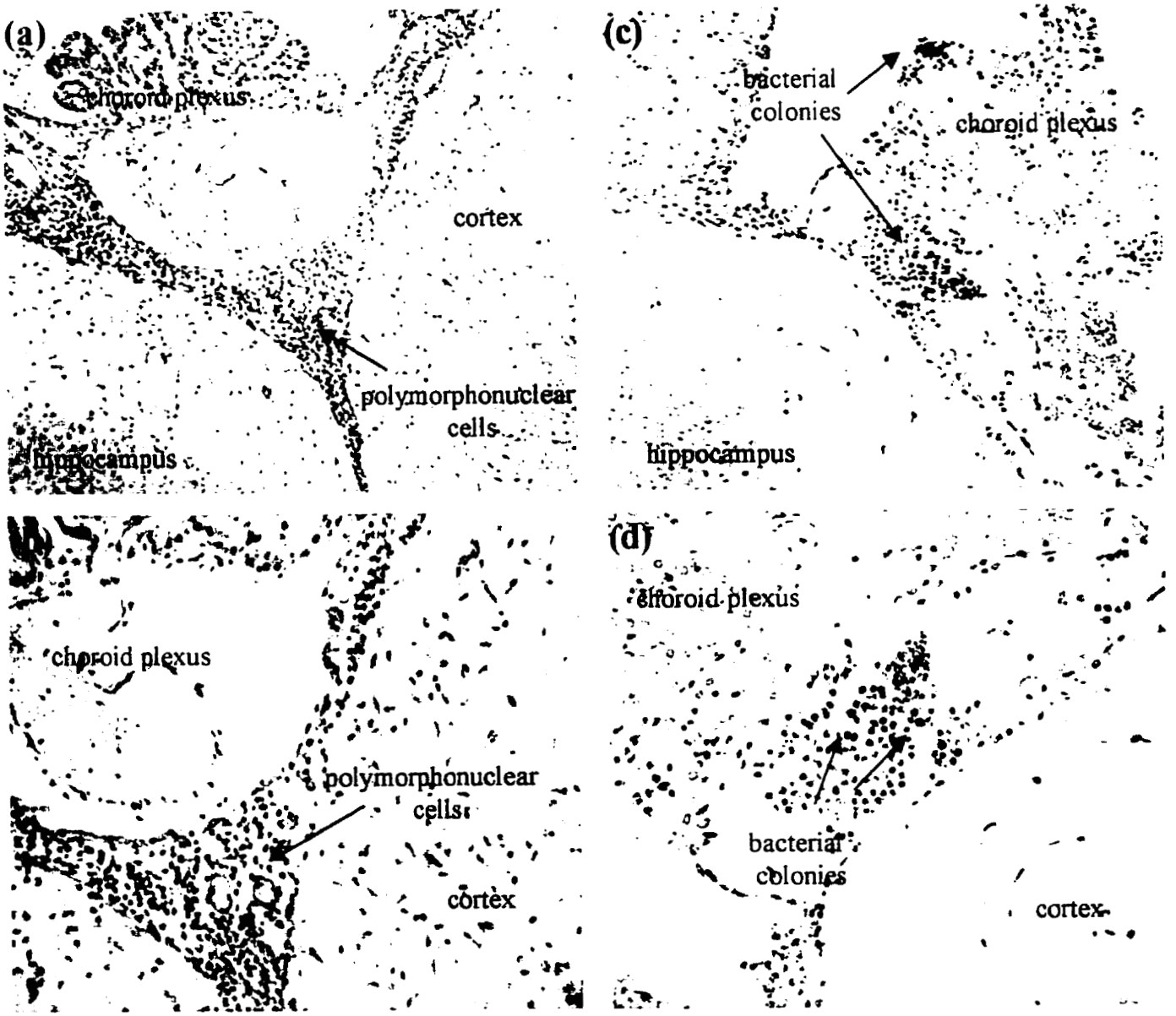
(a)
choroid plexus
cortex
polymorphonuclear cells
hippocampus
(c)
bacterial colonies
choroid plexus
hippocampus
(b)
choroid plexus
polymorphonuclear cells
cortex
(d)
choroid plexus
bacterial colonies
cortex

3.10. Effects of reovirus infection in intracranial 9L gliomas

To determine the effect of reovirus on 9L gliomas implanted intracranially, 5 x 10^4 cells were implanted stereotactically into Fischer 344 rats. Animals receiving a single injection of 5 x 10^4 tumor cells alone, with no subsequent surgery or virus, were moribund in a predictable and uniform fashion with survival ranging from 21-28 days (Figure 3.17A). The survival results of animals repeatedly administered reovirus (live or dead) are shown in Figure 3.17B. Rats receiving repeated injections of reovirus at 10^9 PFUs/dose died faster than their dead virus-treated counterparts. Seven days after the first injection of reovirus (animals received a dose every 48 hours), 7 of the 14 virus-treated group had died (50%). On day 14 however, two dead virus-treated animals were too weak to survive the repeated administration of anaesthetic and did not wake up after receiving treatment. By day 14, only 1/14 animals (7 %) in the live virus group was still alive (This animal received a total of 6 doses of 10^9 PFUs of reovirus) and on day 17 this animal had to be sacrificed due to consistent weight loss and abnormal unresponsiveness to touch.

Although reovirus treatment decreased animal survival, a dramatic difference in tumor size was evident between the live and dead virus-treated groups (Representative sections of animals sacrificed in pairs on day 10). In the live virus-treated animals, tumor occupied 8 ± 1.7 % of the right brain hemisphere, whereas 52 ± 5.2 % was occupied by tumor in the dead virus-treated group (Figure 3.16C). Histopathological examination of serial sections of the brain from reovirus-treated animals showed a dramatic decrease in tumor cells at the site of tumor implantation. This experiment was done as a "proof of concept". From these experiments we learned that repeated administration of reovirus elicits an oncolytic effect. The optimum dose of virus/schedule and route of its administration (taking into account the effect of repeated anesthesia) however has yet to be determined (LD_{50} = 3 doses/ 1 dose every 48 hours/ 10^9 PFUs of reovirus). Gram staining showed a co-existent bacteria-induced encephalitis to be present in the brains of these animals. Furthermore, meningitis resulting from great numbers of bacteria

populating the subarachnoid space of these animals may have had a dramatic effect on their survival. Whether this bacterial infection was in fact the cause of death of the live virus-treated animals in currently under investigation. Bacterial infection could possibly have been the result of the cannula system where repeated wound opening was required to administer virus through the cannula.

Figure 3.17. Effects of reovirus treatment delivered through a chronic indwelling cannula to 9L cells implanted intracerebrally in Fischer 344 immune-competent rats. (A) Growth curve of 5 x 10^4 9L cells implanted intracerebrally into Fischer 344 rats (n = 3 for each time point). (B) Survival plot for the antitumor capacity of reovirus for 9L gliomas. Animals were injected intracerebrally with 5 x 10^4 9L glioma cells and 3 days later received 5 µl intratumoral injection of reovirus (10^9 PFUs). Live or dead virus was subsequently administered every 48 hours through an implanted cannula until animals became moribund. The rats were killed when uncharacteristically unresponsive to touch (live virus group, n = 14; dead virus group, n = 11). (C) Representative coronal H&E sections of rat brains with 9L tumors administered repeated doses of reovirus. A dramatic difference in tumor size can be seen between the two groups, as 8% ± 1.7 (t-test, p = 0.0036) of the right brain hemisphere was occupied by tumor in the live virus-treated group in comparison to 52% ± 5.2 (t-test, p = 0.0074) in the dead virus-treated group. Histologic analysis of live virus-treated brains showed evidence of meningitis, vasculitis and diffuse encephalitis. Great populations of polymorphs were seen surrounding the injection site as well as in the ventricles (polymorphs present in the choroid plexus) (P). Encephalitis, characterized as such by the presence of perivascular cuffs and microglial nodules, was seen in areas throughout the brain (E). An induced bacterial meningitis was evident following gram staining of the same sections. Bacteria were found present throughout the subarachnoid space of the meninges. A co-existent bacteria-induced encephalitis might also be present in the brains of these animals and whether this infection was in fact caused the death of the live virus-treated animals in currently under investigation. Bacterial infection could possibly have been the result of the cannula system where repeated wound opening was required to administer virus through the cannula.

A.

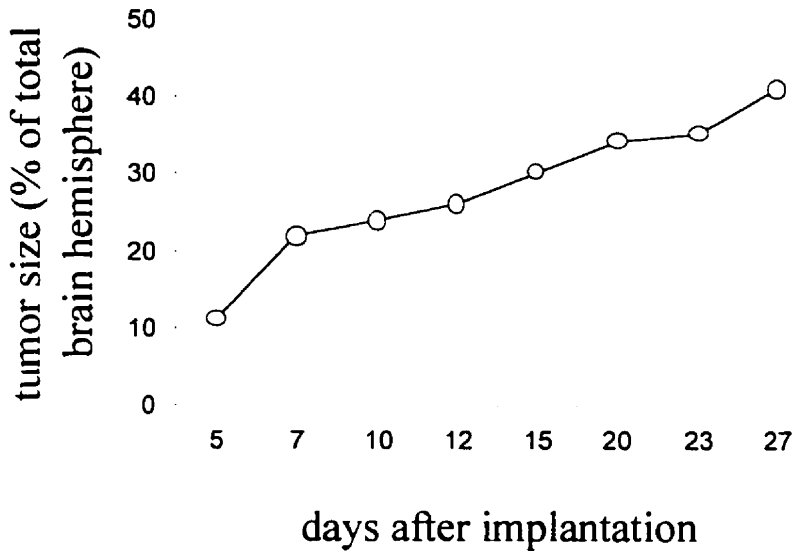
tumor size (% of total brain hemisphere)
50
40
30
20
10
0
5
7
10
12
15
20
23
27
days after implantation

B.

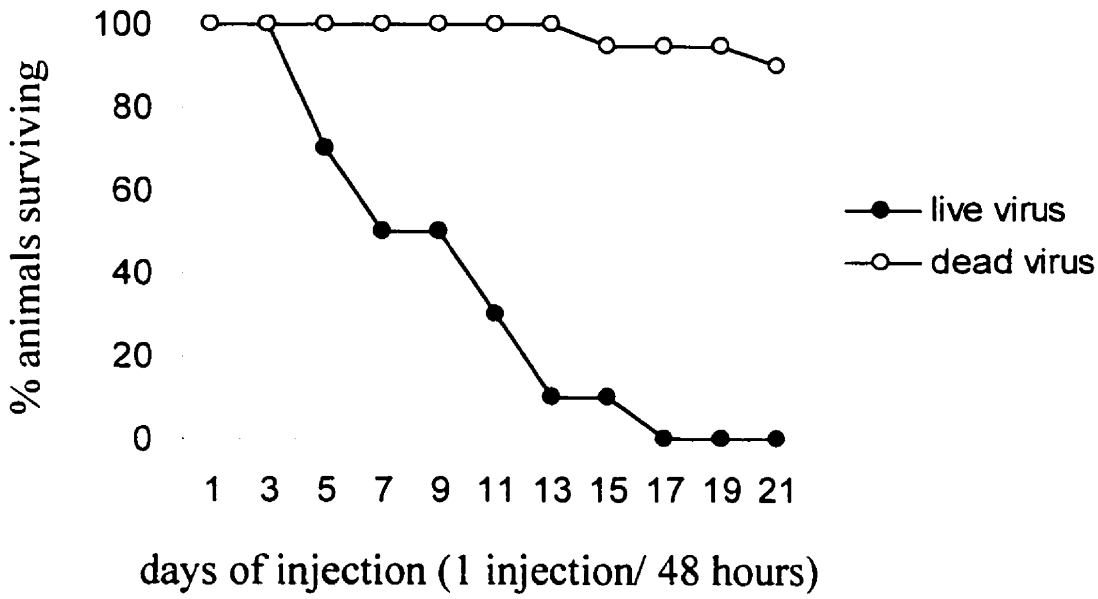
% animals surviving
100
80
60
40
20
0
1
3
5
7
9
11
13
15
17
19
21
days of injection (1 injection/ 48 hours)
live virus
dead virus

C.

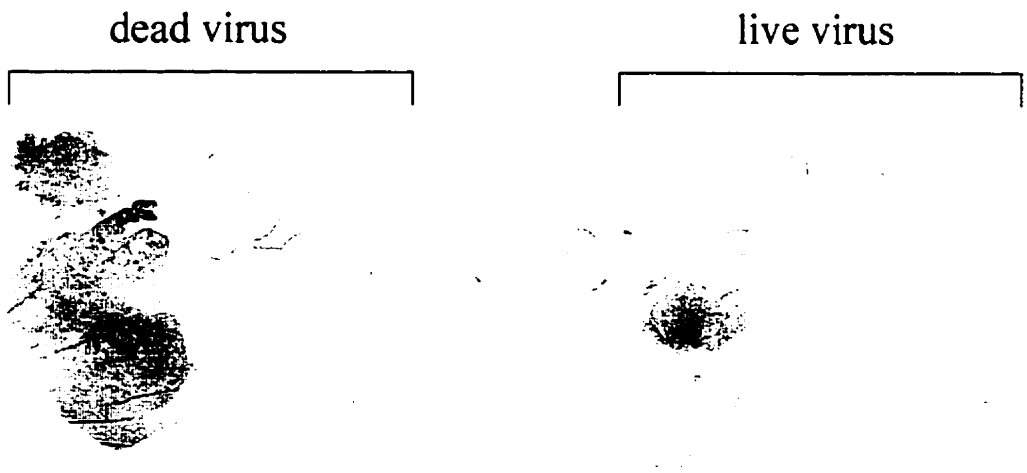
dead virus
live virus

CHAPTER 4: DISCUSSION

This study illustrates the potential benefits and limitations of reovirus as a novel anti-cancer agent for malignant gliomas. Susceptibility of glioma cells to reovirus suggested that: (a) human glioma tumor cells were effectively killed within a 48 hour period by *in vitro* exposure to doses of 40 PFUs/cell in both established cell lines and *ex vivo* glioma specimens; (b) reovirus effectively reduced tumor volume *in vivo* in both subcutaneous and intracerebral SCID NOD models, in most instances curing these mice of their tumors; (c) reovirus caused tumor regression in the presence of pre-existing anti-reovirus antibodies in immunocompetent Fischer rats; (d) reovirus killed tumors remote from the site of administration in immunocompetent hosts; and (e) considerable toxicity was found with this viral approach when repeatedly administered intracerebrally.

The proportion of gliomas potentially treatable by reovirus may be high, even though the number of glioma lines/specimens we tested was small. 80% of the lines tested were susceptible to reovirus infection. A single injection of reovirus caused dramatic tumor regression of human U87 and U251N malignant glioma xenografts in SCID immunodeficient mouse models. Reovirus also caused marked tumor regression in an intracerebral model of human malignant glioma. The percentage of total brain occupied by tumor size was dramatically different between the live and dead virus treated groups (U251N: 38.3% vs. 3.2%; t-test, $p = 0.0026$. U87: 2.4% vs. 40.5%; t-test, $p = 0.0048$) as the oncolytic effects of reovirus were comparable against both U87 and U251N tumors.

The ability of reovirus to infect 9L tumor cells allowed us to assess the efficacy of reovirus treatment in an immunocompetent host. This was important since the majority of human adults have neutralizing antibodies to the virus that could potentially interfere with oncolysis at both a systemic and local level. More frequent reovirus injections were required in an immunocompetent host to achieve similar regression to that in SCID NOD mice and no side effects were seen. In addition, previous exposure to reovirus and the presence of circulating anti-reovirus antibodies did not prevent regression of solid tumors. The presence of these antibodies therefore would not preclude the administration

of virus through a systemic route, as tumor regression was seen even when virus was administered at distant sites. This would suggest that reovirus could attack and kill remotely invasive tumor cells in glioma patients or distant metastases in systemic cancer patients despite the presence of an intact immune system or circulating anti-reovirus antibodies. It is important to note that the level of antibody present in these animals was not titrated. It is therefore possible that differences could exist in the efficacy of reovirus treatment depending on the concentration of circulating antibodies. In these experiments only the presence of circulating antibodies was determined and as such the results obtained are limited in their interpretation as higher antibody titers may or may not abrogate the effects of the virus.

As expected, we found considerable toxicities with reovirus in severely immunocompromised mice. It is pathogenic in neonatal (Tyler and Fields, 1996) and SCID NOD mice (Sherry et al., 1993) but is not known to cause disease in human adults. Various case reports have described **associations** between reovirus infection and a number of diseases (e.g. encephalomyelitis, meningoencephalitis, motor neuron disease, and pneumonitis) but its role in the pathogenesis of these diseases has not been established or generally accepted (Tyler and Fields, 1990). We knew that the SCID NOD mouse was not an ideal model because of toxicities caused by the virus in that host but it did allow us to study human gliomas. Two major toxicities occurred in SCID NOD mice: 1) In 80% (16/20) mice treated with live virus both hind limbs (i.e. ipsilateral and contralateral, non-tumor bearing limbs) became black and necrotic after 21 days. At this time the tumors had regressed and possibly been "cured". We initially wondered if this toxicity was specific for the U87 cell line but it was also seen with the U251N cell line and the breast cancer cell line MDMBA468. Histological analysis of the affected limbs showed what could be a necrotizing vasculitis, but at present, this toxicity has not been properly characterized nor its mechanism determined. 2) All live virus-treated SCID NOD animals, both in the subcutaneous and intracerebral models of glioma, developed focal myocarditis. Inflammation however was not prominent. Myocarditis induced by reovirus consisted acutely of scattered polymorphonuclear cells and then subsequently of lymphocytes and macrophages later in infection. We are encouraged that we do not

however find these toxicities when we use the less immunocompromised nude mouse. No toxicities were encountered in immunocompetent mice or rats. Nevertheless we do not know however whether glioma patients, who are at least mildly immunocompromised (due to impaired cytotoxic responses and the common use of corticosteroids in these patients), will also experience these major toxicities.

A major potential limitation of this approach for glioma patients is the fatal encephalitis seen in immunocompetent rats when it was administered intracerebrally with repeated inoculations. Our preliminary data showed the anti-tumor activity of reovirus against gliomas in immunocompetent rats was impressive but the animals died from presumably from a co-existent bacteria-induced encephalitis however this is a matter of on-going investigation. Therefore, the major question raised is whether these toxicities can be modified while preserving the potent oncolytic properties of reovirus.

Future studies should examine: **1) the optimal dose/schedule of administration.** For example, is there a "therapeutic window" between its oncolytic dose and that which would be fatal? **2) different modes of administration.** The effects of intravenous (i.v.) and intranasal administration on i.c. gliomas is being studied. It will be determined if, for example, reovirus administered i.v. will be able to cross the blood brain barrier and kill gliomas. The intact blood brain barrier in the normal brain may prevent the encephalitis from occurring. **3) The use of less neurovirulent type 3 variants.** Such type 3 variants have been found to induce T cell responses characteristic of reovirus but were unable to invade the CNS of neonatal mice when inoculated into a peripheral site having altered capacity to injury selected parts of the brain (Spriggs et al., 1983). If these variants prove capable of glioma oncolysis and are less neurovirulent, then they might be better candidates for intracerebral inoculation than wild type. Whether these variants would prove effective at killing gliomas or reduce brain injury following repeated administration has yet to be determined. **4) The use of protective anti-reovirus monoclonal antibodies on the prevention of viral pathogenesis.** The administration of specific anti-reovirus antibodies might also prevent or reduce the diffuse encephalitis seen with intracerebral inoculation. Monoclonal antibodies have been shown to inhibit different

stages of reovirus type 3 pathogenesis in the CNS (Tyler et al., 1989). A monoclonal antibody to the type 3 σ1 protein administered by footpad inoculation 24 hrs following virus inoculation was found to "save" neonatal NIH Swiss mice previously killed by reovirus infection (Tyler et al., 1989). This antibody, called σ1mAbG5 was found to eliminate neuronal necrosis as well as significantly attenuate the initial inflammatory response induced by reovirus type 3 in the brain (Tyler et al., 1989). 5) Different reovirus serotypes as anti-glioma agents have yet to be investigated. Reovirus type 1 Lang may also have innate oncolytic capabilities (preliminary observations) against gliomas but may not cause the same lethal, diffuse encephalitis. Reovirus types 1 and 3 have different CNS cell tropisms and therefore they have distinct patterns of virulence (Tyler et al., 1986; Spriggs et al., 1983; Tyler and Fields, 1990). Reovirus type 3 when inoculated into newborn mice causes acute encephalitis that is uniformly fatal and causes the destruction of neuronal cells (Margolis et al., 1971). In contrast, intracerebral inoculation of reovirus type 1 produces a non-fatal infection of ependymal cells that line the ventricular cavities of the brain, with little or no effect on neurons. Hydrocephalus often develops however with reovirus type 1 inoculation, as a consequence of ependymal cell damage (Kilham and Margolis, 1969; Weiner et al., 1980). Whether repeated inoculation of reovirus type 1 into the brain of immunocompetent animals will successfully kill gliomas and not cause any short- or long-term toxicity has yet to be determined.

A single injection (10^9 PFUs) of reovirus was found not to cause any short- or long-term effects on the integrity of brain tissues but repeated injections of reovirus at this dose were lethal (LD_{50} = 3 doses/ 1 dose every 48 hours/ 10^9 PFUs of reovirus). Histological examination of repeatedly inoculated brains showed diffuse encephalitis which we presumed was induced by reovirus infection. While small regions of peritumoral encephalitis would likely be tolerated, and possibly benefit the attack on invasive tumor cells, a diffuse encephalitis would likely be lethal. Obviously this is of great clinical importance.

Ultimately, we expect reovirus to be effective in tumor-bearing immunocompetent rats inoculated intracerebrally as long as toxicities can be minimized by different

doses/schedules, less neurovirulent strains or protective anti-reovirus specific antibodies. The mode of administration is bothersome and may not be directly clinically applicable as virus could be administered through an Ommaya reservoir if appropriate. Ideally reovirus treatment needs to be modified to maximize its cytotoxic ability and then evaluated in appropriate glioma animal models.

There are several limitations to our model as it is not practical to frequently inject rats using the cannulation system. Operative mortality resulting from repeated anesthesia and/or difficulties in virus administration to the same intracerebral location are of concern. Furthermore, this model is not entirely representative of gliomas in patients. It is however commonly accepted and used.

As previously described (Coffey et al., 1998) we found a strong, but not perfect correlation between host infectibility and a high basal level of MAPK activity. MAPK activity was used an indicator of Ras pathway activation. 90% of the cell lines and all (100%) of the glioma surgical specimens found to be susceptible to reovirus infection had high levels of MAPK activity. As expected, other brain tumors (U118, U373, 7 meningiomas and 1 metastatic lung carcinoma specimen) had low MAPK activity and were not susceptible to reovirus infection. Interestingly, two glioma cells (U343 and SF126) showed low MAPK activity and were clearly susceptible to reovirus oncolysis. We have been unsuccessful as yet in testing the hypothesis that MAPK activation is critical for *in vivo* oncolysis since tumors with low MAPK activity will not form tumors in mice. The precise mechanism behind the selective replication of reovirus in low MAPK cells has yet to be determined since it may involve the activation of parallel signaling pathways. There is some evidence to suggest that activation of the JNK stress pathway may be required for infection in low MAPK cells.

Other promising oncolytic viruses that have gained notoriety would include the EB1 gene attenuated adenovirus ONYX-015 (Bischoff et al., 1996; Heise et al., 1997) and the genetically altered herpes simplex virus G207 (Toda et al., 1998; Toda et al., 1999; Hunter et al., 1999). Advantages as well as shortcomings exist for each of these viral

therapies. Firstly, while each of these three viruses are relatively benign, both ONYX-015 and G207 are genetically engineered (Bischoff et al., 1996; Martuza et al., 1991) whereas the reovirus used here is a laboratory strain (since 1959) whose genetic make-up has never been intentionally tampered with (Tyler and Fields, 1996). Whether recent field isolates of reovirus have similar oncolytic capability remains to be seen. Secondly, ONYX- 015 targets cancer cells lacking functional tumor suppressor protein p53 (mutant p53 is found in over half of all human cancers) (Leco, 1992; Bischoff et al., 1996), G207 has been genetically altered to target cancer cells with a dysfunctional p16/pRB tumor suppressor pathway (Chase et al., 1998) whereas reovirus targets tumors with an activated Ras signaling pathway (Strong et al., 1998). The importance of this mechanistic distinction is exemplified by the demonstration that the U87 glioblastoma cell lines, which contains functional p53 but over-expresses PDGF-R, is resistant to ONYX-015 (Bischoff et al., 1996) but is highly sensitive to reovirus treatment. Lastly, previous studies using animal models with either ONYX-015 and G207 in the brain has shown impressive anti-tumoral efficacy but the long-term inflammatory effects of such treatments have yet to be determined and therefore current clinical trials for human gliomas using these vectors are of concern. The long-term consequences of adenovirus-mediated conditional cytotoxic gene therapy for the treatment of malignant gliomas remains largely uncharacterized. The induction of chronic inflammation by this vector, consequent to tumor eradication in mice, has been found to influence the functional integrity of brain parenchyma (Kielian and Hickey, 1999). Further, this phenomenon has not been limited to adenovirus vectors. Strong and widespread immunoreactivity has been seen in large areas of rodent brains following herpes-simplex virus-1-thymidine kinase treatment (HSV-1-tk) (Dewey et al., 1999; Kielian and Hickey, 1999). Despite tumor eradication, chronic active inflammation has been demonstrated by the presence of macrophages and CD8+ T cells at the original tumor site, in addition to microglia and astrocyte activation in the brain following Adv/HSV-1-TK (gancyclovir) suicide therapy (Kielian and Hickey, 1999). Furthermore, this active inflammation was found to persist three months following the successful inhibition of glioma growth in a syngeneic rodent glioma model (Kielian and Hickey, 1999). These findings are of major concern, as it remains to be determined if reovirus inoculation in the brains of immunocompetent

animal models, or in patients, will have similar long-term toxicities. We are currently determining the efficacy and toxicity of reovirus in immunocompetent (i.e. intracerebral) brain tumor models.

The potential short- and long-term effects of reovirus administration in the brain are currently under investigation. Whether chronic active inflammation, seen in both G207 and ONYX-015 therapeutic models, will be a consequence of reovirus oncolysis of gliomas has yet to be determined. Our study does suggest however that reovirus with its relatively mild pathogenicity and potent oncolytic activity against glioma tumors warrants further investigations that could lead to future clinical trials for malignant gliomas. Following the assessment of its toxicity in the brain, reovirus would be a strong candidate to be used in combination with other conventional therapies as whether or not such treatments as chemotherapy for example will augment the anti-cancer effects of reovirus has yet to be determined.

LITERATURE CITED

Bassel-Duby R, DR Spriggs, KL Tyler and BN Fields. 1986. Identification of attenuating mutations on the reovirus type 3 S1 double-stranded RNA segment with a rapid sequencing technique. J Virol 60: 64-67.

Bellemy AR and WK Joklik. 1967. Studies on reovirus RNA II. Characterization of reovirus messenger RNA and of the genome RNA segments from which it is transcribed. J Mol Biol 29; 19-26.

Chase M, RY Chung and EA Chiocca. 1998. An oncolytic viral mutant that delivers the CYP2B1 transgene and augments cyclophophamide chemotherapy. Nature Biotechology 16: 444-448.

Choi AHC, RW Paul and PWK Lee. 1990. Reovirus binds to multiple plasma membrane proteins on mouse L fibroblasts. Virology 178: 316-320.

Clemens MJ and A Elia. 1997. The Double-Stranded RNA-Dependent Protein Kinase PKR: Structure and Function. J of Interferon and Cytokine Research 17; 503-524.

Coffey MC, Strong JE, Forsyth PA and PWK Lee. 1998. Reovirus as An agent Against Tumors with Activated Ras Pathway. Science 282; p.1132-1134.

DeHaro C, R Mendez and J Santoyo. 1996. The eIF-2a kinases and the control of protein synthesis. FASEB J 10: 1378-1387.

Detjen BM, WE Walden and RE Thach. 1982. Translational specificity in reovirus-infected mouse fibroblasts. J Biol Chem 257: 9855-9860.

Dewey RA, G Morrissey, CM Cowsill, D Stone, F Bolonani, NJ Dodd, TD Southgate, D Klatzmann, H Lassman, MG Castro and PR Lowenstein. 1999. Chronic brain inflammation and persistent herpes simplex virus 1 thymidine kinase expression in survivors of syngeneic glioma treated by adenovirus-mediated gene therapy: implications for clinical trials. Nature Medicine 5: 1256-63.

Duncan MR, Stanish SM and DC Cox. 1978. Differential sensitivity of normal and transformed human cells to reovirus infection. J Virol 28; 444-449.

Ekstrand AJ, N Longo, ML Hamid, JJ Olson, L Lui, VP Collins and CD James. 1994. Functional characterization of EGF receptor with a truncated extracellular domain expressed in glioblastomas with EGF-R gene amplification. Oncogene 9: 2313-2320.

Ekstrand AJ, N Sugawa, C James and V Collins. 1992. Amplified and rearranged epidermal growth factor receptor genes in human glioblastomas reveal deletions of sequences encoding portions of the N- and/or C-terminal tails. PNAS USA 89: 4309-4313.

Flamand A, J-P Gagner, LA Morrison and BN Fields. 1991. Penetration of the Nervous systems of suckling mice by mammalian reoviruses. J Virol 65: 123-131.

Forsyth PA, Cairncross JG. 1995. Treatment of malignant glioma in adults. Current Opinion Neurology 8: 414-418.

Gentsch JR and AF Pacitti. 1985. Effect of neuraminidase treatment of cells and effect of soluble glycoproteins on type 3 reovirus attachment to murine L cells. J Virol 56: 356-364.

Gentsch JR and AF Pacitti. 1987. Differential interaction of reovirus type 3 with sialylated receptor components on animal cells. Virology 161; 245-248.

Gerosa MA, D Talarico, C Fognani, E Raimondi, M Colombatti, G Tridente, L De Carli and G Della Valle. 1989. Over expression of N-ras oncogene and EGFR gene in human glioblastomas. J National Cancer Institute. 81(1): 63-67.

Giorgi C, BM Blumberg and D Kolakofsky. 1983. Sendai Virus contains overlapping genes expressed from a single mRNA. Cell 35: 829-836.

Gonzales MF. 1995. Brain Tumors. Chapter 3. *Edited by* AH Kay and ER Laws. Churchill Livingstone, New York.

Guha A, Dashner K, Black P, Wagner J, Stiles C. 1995a. Expression of PDGF and PDGFRs in human astrocytoma operative specimens. Int J Cancer 16: 168-173

Guha A, Gowacka D, Carrol R, Dashner K, Black PM, Stiles CD. 1995b. Expression of platelet derived growth factor and platelet derived growth factor receptor in human glial tumors. Cancer Res 52; 4550-4553.

Guha A. 1998. Ras Activation in Astrocytomas and Neurofibromas. Can J Neurol Sci 25: 267-281.

Guha A. 1992. Platelet derived growth factor: A general review with emphasis on astrocytomas. Pediatric Neurosurgery 92:17;14-20.

Haller BL, ML Barkon, X-Y Li, WM Hu, JD Wetzel, TS Dermody and HW Virgin IV. 1995a. Brain- and Intestine-Specific variants of reovirus serotype 3 strain Dearing are selected during chronic infection of severe combined immunodeficient mice. J Virol 69: 3993-3937.

Haller BL, ML Barkon, GP Vogler and HW Virgin IV. 1995b. Genetic mapping of reovirus virulence and organ tropism in severe combined immunodeficient: organ-specific virulence genes. J Virol 69: 357-364.

Hashiro G, Loh PC, JT Yau. 1977. The preferential cytotoxicity of reovirus for certain transformed cell lines. Arch Virol 54; 302-315.

Helseth E, G Unsgaard, A Dalen, H Fure, T Skandsen, A Odegaard and R Vik. 1988. Amplification of the EGFR gene in biopsy specimens from human intracranial tumors. British J of Neurosurgery 2(2): 217-225.

Hovanessian AG. 1989. The Double Stranded RNA-Activated Protein Kinase Induced by Interferon: dsRNA-PK. J of Interferon Research 9: 641-647.

Hurtt MR, J Moosy, M Donovan-Peluso and J Locker. 1992. Amplification of EGFR gene in gliomas: histopathology and prognosis. J of Neuropathology & Experimental Neurology 51(1): 84-90.

Imai M, MA Richardson, N Ikegami, AJ Shatkin and Y Furuichi. 1983. Molecular cloning of double-stranded RNA virus genomes. PNAS 80: 373-377.

James C and V Collins. 1992. Molecular genetic characterization of CNS tumor oncogenesis. Adv Can Res 58: 121-142.

James C, E Carlbom and JP Dumanski. 1988. Clonal genomic alterations in glioma malignancy stages. Cancer Res 48: 5546-5551.

Joklik WK. 1985. Recent progress in reovirus research. Annual Rev Genetics 19; 537-575.

Kamb A, NA Gruis, J Weaver-Feldhaus ET AL. 1994. A cell cycle regulator potentially involved in genesis of many tumor types. Science 264: 436-440.

Kielian T and WF Hickey. 1999. Inflammatory thoughts about glioma gene therapy. Nature Medicine 5(11): 1237-1238.

Kumabe T, Y Sohma, T Kayama, T Yoshimoto and T Yamamoto. 1992. Over expression and amplification of alpha-PDGFR gene lacking exons coding for a portion of the extracellular region in a malignant glioma. J Experimental Medicine 168(2): 265-269.

Laemmli, UK. 1970. Cleavage of structural proteins during the assembly of the head of bacteriophage T4. Nature (London) 277: 680-685.

Laing FF, Miller DC and M Koslow. 1994. Pathways leading to glioblastoma multiformes: a molecular analysis of genetic alterations in 65 astrocytic tumors. J Neurosurg 81; 427-436.

Lee PWK, Hayes EC, WK Joklik. 1981. Protein sigma 1 is the reovirus cell attachment protein. Virology 108; 156-163.

Lemay G. 1988. Transcriptional and translation events during reovirus infection. Biochem Cell Biol 66: 803-812.

Li D-M and H Sun. 1997. TEP1, encoded by candidate tumor suppressor locus, is a novel protein tyrosine phosphatase regulated by transforming growth factor-b. Cancer Res 57: 2124-2129.

Li J, C Yen, D Liaw, K Podsypanina, S Bose, SI Wang, J Puc, C Miliarsis, L Rodgers, R McCombie, SH Bigner, BC Giovanella, M Ittmann, B Tycko, H Hibshoosh, WH Wigler and R Parsons. 1997. PTEN, a putative protein tyrosine phosphatase gene mutated in human brain, breast and prostate cancer. Science 275: 1943-1947.

Libermann T and N Razon. 1984. Expression of EGF receptors in human brain tumors. Cancer Res 44: 753-760.

Libermann T, H Nusbaum and N Razon. 1985. Amplification, enhanced expression and possible rearrangement of EGF-receptor gene in primary human tumors of glial origin. Nature 313: 144-147.

Luftig RB, S Kilham, AJ Hay, HJ Zweerink and WK Joklik. 1972. An ultra structure study of virions and cores of reovirus serotype 3. Virology 48; 170-178.

Munemitsu SM and CE Samuel. 1984. Biosynthesis of reovirus specified polypeptides: multiplication rate but not yield of reovirus serotype 1 and 3 correlates with the level of virus-mediated inhibition of cellular protein synthesis. Virology 136: 133-143.

Munoz A, MA Alonso and L Carrasco. 1985. The regulation of translation in reovirus-infected cells. J Gen Virol 66: 2161-2170.

Nibert ML, Schiff LA, Fields BN. 1996. Reoviruses and their replication. In:Virology, eds. Fields BN, Knipe DM, Howley PM, Chanock RM, Melnick JL, Monath TP, Roizman B. Lippincott-Raven Press, Philadelphia, pp. 1557-1597.

Nister M, L Claesson-Welsh, A Eriksson, CH Heldin and B Westermark. 1991. Differential expression of PDGFR in human malignant glioma cell lines. J of Biological Chemistry 266(25): 16755-63.

Nobori T, K Miura K, DJ Wu, A Loys, K Takabayashi and DA Carson. 1994. Deletions of cyclin-dependent kinase-4 inhibitor gene in multiple human cancers. Nature (London) 368: 753-756.

Paul RW, AH Choi and PWK Lee. 1989. The α-anomeric form of sialic acid is the minimal receptor determinant recognized by reovirus. Virology 172: 382-385.

Perhouse MA, E Stubblefield, A Hadi, AM Killary, WKA Yung and PA Steck. 1993. Analysis of the functional role of chromosome 10 loss in human glioblastomas. Cancer Res 53: 5043-5050.

Reifenberger G, Liu L, and K Ichimura. 1993. Amplification and over expression of the MDM2 gene in a subset of human malignant gliomas without p53 mutations. Cancer Res 53; 2736-2739.

Rosen L. 1960. Serologic grouping of reoviruses by hemagglutination-inhibition. Am J Hyg 71; 242-249.

Rubin DH and BN Fields. 1980. Molecular basis of reovirus virulence: role of the M2 gene. J Exp Med 152; 853-868.

Rubio M-P, KM Correa, K Ueki, HW Mohrenweiser, JF Gusella, A von Deimling and DN Louis. 1994. Putative glioma tumor suppressor gene in chromosome 19q maps between APOC2 and HRC. Cancer Res 54: 4760-4763.

Sabin AB. 1959. Reoviruses. Science 130; 1387.

Scott JN, NB Rewcastle, PMA Brasher, D Fulton, JA MacKinnon. M Hamilton, JG Cairncross and PAJ Forsyth. 1999. Which Glioblastoma Multiforme Patient will Become a Long-Term Survivor? A Population Based Study. Annals of Neurology 46: 183- 188.

Sharpe AH and BN Fields. 1982. Reovirus inhibition of cellular RNA and protein synthesis: role of the S4 gene. Virology 122: 381-391.

Sharpe, AH and BN Fields. 1985. Pathogenesis of viral infections: Basic concepts derived from the reovirus model. N Engl J Med. 312: 486-497.

Shatkin AJ, Sipe JD, and PC Loh. 1968. Separation of tem reovirus genome segments by polyacrylamide gel electrophoresis. J Virol 2; 986-991.

Shaw JE and DC Cox. 1973. Early inhibition of cellular DNA synthesis by high multiplicities of infectious and UV-inactivated reovirus. J Virol 12: 704-710.

Smith RE, HJ Zweerink and WK Joklik. 1969. Polypeptide components of virions, top component and cores of reovirus type 3. Virology 39: 791-810.

Spriggs DR, RT Bronson and BN Fields. 1983. Hemagglutinin variants of reovirus type 3 have altered central nervous system tropism. Science 220: 505-507.

Stanley NF and PJ Leak. 1963. Murine infection with reovirus type 3 and the runting syndrome. Nature 199: 1309-1310.

Steck P, MA Perhouse and SA Jasser. 1997. Identification of a candidate tumor suppressor gene, MMAC1, at chromosome 10q23.3 that is mutated in multiple advanced cancers. Nature Genetics 15: 356-362.

Steck P, P Lee, M-C Hung and W Yung. 1988. Expression of an altered epidermal growth factor receptor by human glioblastoma cells. Cancer Res 48: 5433-5439.

Strong JE and PWK Lee. 1996. The v-erbB oncogene confers enhanced cellular susceptibility to reovirus infection. J Virol 70; 612-616.

Strong JE, Coffey MC, Tang D, Sabinin P and PWK Lee. 1998. The molecular basis of reovirus oncolysis: usurpation of the Ras signaling pathway by reovirus. EMBO J 17; 12: 3351-3362.

Strong JE, Tang D and PWK Lee. 1993. Evidence that the EGFR on host cells confers reovirus infection efficiency. Virology 197; 405-411.

Tatter SB and GR Harsh IV. 1998. Current Treatment Modalities for Brain Tumors: Surgery, Radiation and Chemotherapy. *In* Gene Therapy for Neurological Disorders and Brain Tumors. *Edited by* EA Chiocca and XO Breakefield. Humana Press: Totowa, New Jersey. 161-190.

Toda M, SD Rabkin and RL Martuza. 1998. Treatment of human breast cancer in brain metastatic model by G207, a replication-competent multimutated herpes simplex virus 1. Human Gene Therapy 9: 2177-2185.

Toda M, SD Rabkin H Kojimaand RL Martuza. 1999. Herpes simplex virus as an in situ cancer vaccine for the induction of specific anti-tumor immunity. Human Gene Therapy 10: 385-393.

Tyler K, Fields BN. 1996. Reoviruses. In:Virology, eds. Fields BN, Knipe DM, Howley PM, Chanock RM, Melnick JL, Monath TP, Roizman B. Lippincott-Raven Press, Philadelphia, pp. 1597-1663.

Tyler KL and BN Fields. 1990. Reoviridae: A Brief Introduction. In:Virology, ed. Fields. BN. Raven Press, New York, pp. 1271-1273.

VonDeimling A, R Eibl, H Ohgaki, DN Louis, K von Ammon, I Petersen, P Kleihues, RY Chung and OD Wiestler. 1992. p53 mutations are associated with 17q allelic loss in grade II and grade III astrocytoma. Cancer Res 52: 2987-2990.

Weiner HL and WK Joklik. 1989. The sequences of the reovirus serotype 1, 2, and 3 L1 genome segments and analysis of the mode of divergence of the reovirus serotypes. Virology 169: 194-203.

Weiner HL, ML Powers and BN Fields. 1980. Absolute Linkage of Virulence and CNS cell Tropism of Reoviruses to Viral Hemagglutinin. J of Inf Diseases 141: 609-616.

Yue Z and AJ Shatkin. 1997. Double-stranded RNA-dependent protein kinase (PKR) is regulated by reovirus structural proteins. Virology 234: 364-371.

Zarbl H and S Millward. 1983. The reovirus multiplication cycle. *In* The reoviridae. *Edited by* WK Joklik. Plenum Publishing Corporation, New York, London. 107-196.

Zweerink HJ and WK Joklik. 1970. Studies on the intracellular synthesis of reovirus specified proteins. Virology 41: 501-518.